NATO STANDARD

AEP-96

THE SIX/SEVEN DEGREES OF FREEDOM GUIDED PROJECTILE TRAJECTORY MODEL

Edition A Version 1

MAY 2016

NORTH ATLANTIC TREATY ORGANIZATION

ALLIED ENGINEERING PUBLICATION

Published by the
NATO STANDARDIZATION OFFICE (NSO)

INTENTIONALLY BLANK

NORTH ATLANTIC TREATY ORGANIZATION (NATO)

NATO STANDARDIZATION OFFICE (NSO)

NATO LETTER OF PROMULGATION

17 May 2016

1. The enclosed Allied Engineering Publication AEP-96, Edition A, Version 1 THE SIX/SEVEN DEGREES OF FREEDOM GUIDED PROJECTILE TRAJECTORY MODEL, which has been approved by the nations in the NATO Army Armaments Group, Integrated Capability Group Indirect Fire, is promulgated herewith. The agreement of nations to use this publication is recorded in STANREC 4618.

2. AEP-96, Edition A, Version 1 is effective upon receipt.

3. No part of this publication may be reproduced, stored in a retrieval system, used commercially, adapted, or transmitted in any form or by any means, electronic, mechanical, photo-copying, recording or otherwise, without the prior permission of the publisher. With the exception of commercial sales, this does not apply to member or partner nations, or NATO commands and bodies.

4. This publication shall be handled in accordance with C-M(2002)60.

Edvardas MAŽEIKIS
Major General, LTUAF
Director, NATO Standardization Office

INTENTIONALLY BLANK

RESERVED FOR NATIONAL LETTER OF PROMULGATION

INTENTIONALLY BLANK

TABLE OF CONTENTS

INTENTIONALLY BLANK

1 AIM

1.1 The principal aim of this agreement is to standardize the Six/Seven Degrees of Freedom (DOF) Guided Projectile Trajectory Model for exterior ballistics trajectory simulation of artillery projectiles for the NATO Naval and Army Forces. This will facilitate the development of simpler variants for use in fire control systems and the exchange of exterior ballistics data and fire control information.

1.2 RELATED DOCUMENTS

STANAG 4106	Procedures to Determine the Degree of Ballistic Performance Similarity of NATO Indirect Fire Ammunition and the Applicable Corrections to Aiming Data
STANAG 4119	Adoption of a Standard Cannon Artillery Firing Table Format
STANAG 4144	Dynamic Firing Technique to Determine Ballistic Data for Cannon Artillery Firing Tables and Associated Fire Control Equipment
STANAG 4355	The Modified Point Mass and Five Degrees of Freedom Trajectory Models
STANAG 4683	NATO Technical Sharable Software (NTSS)
AOP 61	NATO Technical Sharable Software (NTSS) - Product Development Standards and Guidelines
ISO 2533-975(E)	The ISO Standard Atmosphere
STANAG 6022	Adoption of a Standard Gridded Data Meteorological Message

2 AGREEMENT

Participating nations agree to use the Six/Seven Degrees of Freedom Guided Projectile Trajectory Model for exterior ballistics trajectory simulation of spin-stabilized and fin-stabilized guided projectiles with or without rocket assist or base burn assist, as an adjunct to STANAG 4355.

3 GENERAL

This agreement permits some flexibility by accommodating certain specific national aerodynamic conventions and ballistic data analysis procedures.

4 DETAILS OF THE AGREEMENT

The details of the agreement are given hereunder and are divided into the following four parts:

4.1 Elements Of A Six/Seven Degrees Of Freedom Simulation

This document sets up the STANREC for a mathematical model representing the flight of a spin- stabilized or fin-stabilized, conventional or guided, artillery projectile. The 6 degrees of freedom of a rigid body are comprised by the three components of the linear velocities of the center of mass (in both inertial coordinates and body coordinates) and the three components of the angular velocity vector $\overline{\omega}$ with respect to the center of mass (body coordinates). Sometimes a seventh degree of freedom is required to model a projectile which consists of two rigid bodies. The seven degrees of freedom trajectory model is limited to dual-spin projectiles. Thus, the two bodies are coaxial in pitch and yaw, as if a single body, but can spin independently. The seventh degree of freedom is defined as the spin of body 2 with respect to body 1.

Since the equations of motion are second order, there must be two integrations for each degree of freedom. Since there are many aspects of projectile modeling (e.g., aerodynamics, inertial properties, sensor outputs) that are simplest to describe in a coordinate frame that rolls, pitches, and yaws with the projectile and others (e.g., gun and target position, GPS or global positioning system coordinates) that are more conveniently expressed in Earth-centered Earth-fixed (ECEF) coordinates, a hybrid approach is used here. There are two integration frames used, related to each other by a rotation but not a translation. Firstly, consider the accelerations or derivatives of the linear and angular rates ($\dot{U}_x, \dot{U}_y, \dot{U}_z, \dot{p}, \dot{q}$ and $\dot{r}$) in the body integration frame. These are really the ECEF accelerations that are resolved in the angular orientation of the body frame. They are integrated to obtain U_x, U_y, U_z, p, q and r in the same body integration frame. Then the velocity components U_x, U_y and U_z are rotated (not translated) to the ECEF frame where a second integration is carried out to keep track of the projectile's position in ECEF space.

To create a 6 or 7 degree of freedom trajectory simulation of a projectile, the following elements are needed.

4.1.1. Rotation Matrix: Parameters are needed to characterize the relative orientation of the body integration frame for the equations of motion and the Earth frame and to transform between these frames. Quaternion parameters will be used internal to the simulation for the equations of motion. Euler angles will be used for input and output. A rotation matrix that is a function of these parameters is required. See Annex A about coordinate transformations. Note that this matrix rotates but does not translate coordinates.

4.1.2. Body Frame: A body frame is needed that pitches and yaws with the projectile. It may also either spin with the projectile (body-fixed frame) or it may not spin with the projectile (zero-roll frame or zero-spin frame). The coordinate system associated to this frame will be used to express the equations of motion of the projectile and to integrate them with respect to time. For convenience, this frame (and its associated coordinate system) will be called the body integration frame (system) or just body frame (system). See Annex A about reference frames and coordinate systems and section II-1 in the main body of this STANREC.

4.1.3. Equations of Motion: We require equations of motion of the projectile to be expressed in whichever type of body integration system that we are using (body-fixed or zero-roll/spin). Newton's Law for a rigid body will have 3 linear velocity components for the center of mass and 3 angular velocity components about the center of mass, for a total of 6 equations of motion. Some guided projectiles will have forward and aft sections that are coaxial but can spin independently of one another. The additional spin is a seventh degree of freedom and adds a seventh equation of motion. The forward unit is considered primary since it would contain the projectile sensors and controls and would generally be roll stabilized. There are also needed some addition differential equations to give the time development of the four quaternion parameters. They are connected to the equations of motion of the projectile through the components of the angular velocity vector $\overline{\omega}$. These components are conventionally called *p*, *q* and *r* by aerodynamicists. The treatment of the kinematics will be quite general. It is made specific to the projectile through the physical properties, mass and moments of inertia. See section II-2 in this STANREC. Initial conditions and other factors, e.g. thrust for some projectiles, are required.

4.1.4. Projectile Dynamics and Aerodynamics: Projectile dynamics also require models of any reaction motors (rockets) and the aerodynamic coefficients. The principle aerodynamic coefficients are the normal force, pitching and yawing moments, pitch and yaw damping moments, roll and roll damping moments and the axial force. If the projectile is spinning rapidly, Magnus force and Magnus moment coefficients are also needed. The pitching moment may be obtained by multiplying the normal force and the difference between a center of pressure and the center of mass. This difference is the static margin. The aerodynamic coefficients are usually expressed as a multidimensional table with independent variables such as the Mach number, angle of attack, aerodynamic roll angle, control surface deflections and the like. For this reason, a scheme for table look up and interpolation is needed. See Annex B "Projectile Aerodynamics", Annex D - "Additional Terms for Rocket-Assisted and Base-Burn Projectiles - Method 1" and Annex E "Additional Terms for Rocket-Assisted and Base-Burn Projectiles - Method 2".

4.1.5. Atmospheric Modeling: Projectile dynamics require an atmospheric model. Specifically the air density and the virtual temperature are needed. The virtual temperature takes into account the relative humidity of the air: it is the temperature that dry air would have if its pressure and density were equal to those of a given sample of moist air. See STANAG 6022. The virtual temperature is used to calculate the speed of sound, which is needed to find the Mach number. If rocket motors or diverters are present, the air pressure is needed to correct the thrust for altitudes above sea level. The standard atmospheric models of the atmosphere can be used but provision must also be made to utilize data from a “met message” from an actual test or fire control center. “Met” is an abbreviation for meteorological. These met data might be obtained by weather balloons and the treatment must be consistent with the met message format**.** If any two of air density, pressure or temperature are known, the other can be calculated, as can be other parameters that in some cases might be needed, such as the kinematic/dynamic viscosities. The met data is provided in the geodetic system. See Annex A about the reference coordinate systems.

4.1.6. Earth Frame: several coordinate systems can be used to represent the “Earth Frame”. Two systems are of main importance. The first one is the Earth-centered Earth-fixed (ECEF) system that is located at the center of the Earth. The second one is the fire control system that is located at the gun position. Both systems rotate with Earth. See Annex A about the reference coordinate systems and section II-1 in the main body of this STANREC.

4.1.7. Guidance Modeling: For guided projectiles, items such as seekers, accelerometers, inertial rate sensors, autopilot and GNC (guidance, navigation and control) algorithms and the CAS (control actuator system) are required. See Annex F - "Guided Projectile Modeling".

4.1.8. Numerical Integration: Since these equations are too complex to be solved in closed or analytical form, there must be a mechanism for numerical integration of the equations of motion. See Annex G - "Numerical Integration".

4.2 Equations Of Motion

4.2.1. Frames and Coordinate Systems

The fire control system is a right-handed orthonormal Cartesian coordinate system that is attached to the Earth-fixed frame. Its origin is located at the gun position and is needed for aiming. The fire control system is defined by axes 1, 2 and 3 (fig. 1). This is also the coordinate system used in the NABK modified point-mass model defined in STANAG 4355. This six/seven DOF (degrees of freedom) guided projectile simulation also uses an Earth-Centered Earth-Fixed (ECEF) system that is conventional with the ellipsoidal Earth WGS-84 model (with optional geoidal corrections). See Annex A for the detailed description of the Earth reference frames and systems.

The body system is a right-handed orthonormal Cartesian coordinate system defined by axes *x*, *y* and *z* (fig. 1) that is attached to the body frame. This frame is used to describe the projectile inertial properties and aerodynamics and to express and integrate the equations of motion. The body frame is also called the equation of motion (EOM) frame.

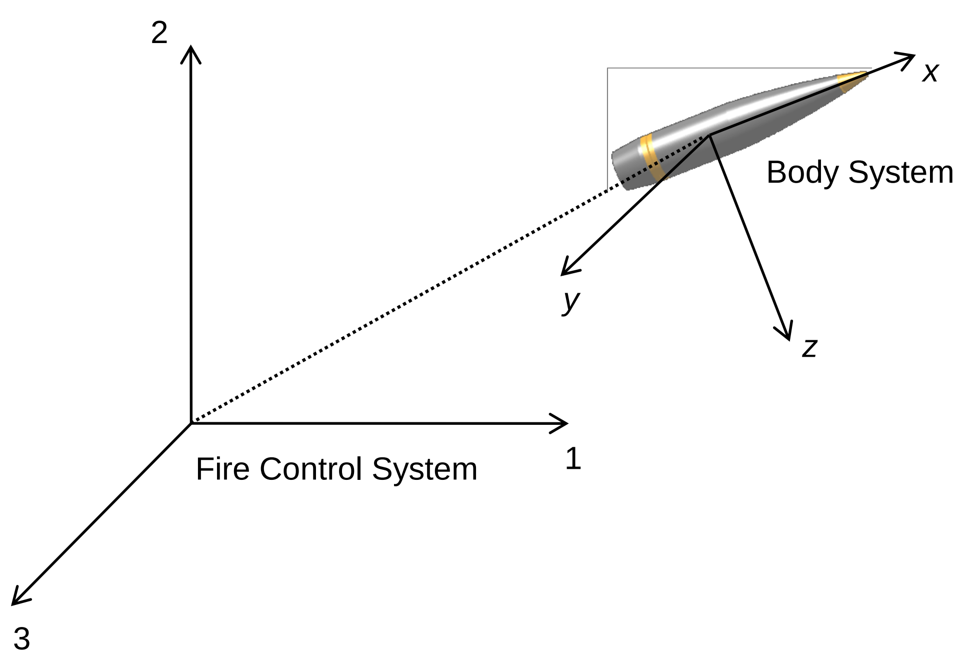

Figure 1: Fire Control and Body Coordinate Systems

The body frame is a rotating frame that may be the body-fixed, the zero-roll or the zero-spin frame. Where, the roll angle of the zero-roll frame is always set to zero, keeping the lateral axis in a fixed plane. The spin rate of the zero-spin frame is always set to zero. It is customary in aerodynamics to refer to the x, y and z components of the angular velocity vector $\overline{\varpi}$ as *p*, *q* and *r*. The body-fixed frame fully rotates with the projectile. Thus, the *p, q* and *r* are the same for projectile body and the frame for integrating the equations of motion. For zero-roll and zero-spin frames, the first component of the frame angular velocity is not equal to the projectile spin *p*. However, the second and third components of the angular velocity of both frames are still equal to the projectile *q* and *r* angular velocities. The reason for this choice of frames is that gravity appears to rotate at the rate of the projectile spin *p* in the body-fixed frame, which significantly reduces the integration time step for spin-stabilized projectiles. In zero-roll and zero-spin frames, the angular velocity of the gravity vector is either zero or very low, which significantly increases the integration time step and speeds up the integration process. However, to maintain the advantage of more efficient integration, the characteristics of the projectile that appear in the equations of motion (such as aerodynamic coefficients and the moment of inertia) must be rotationally symmetric. Spin-stabilized projectiles generally have this symmetry whereas fin-stabilized projectiles generally do not. See Annex A for the detailed description of the body frames and systems.

4.2.2 Equations of Motion

4.2.2.1 Translational and Rotational Equations of Motion

We require equations of motion of the projectile to be expressed in whichever type of integration frame that we are using. These arise from Newton's laws. There are 3 equations for the components of the linear velocity of the center of mass and 3 equations for the components of the vector angular velocity about the center of mass. Sometimes it will be necessary to model a guided projectile in which the front and rear sections are coaxial but can roll independently of one another. The additional spin rate is the seventh degree of freedom and leads to an additional equation. The front section will define the body-fixed coordinate frame because sensors are located in this section and it is generally roll stabilized.

Newton's second law gives the translational equation of motion of the projectile with respect to the Earth-Centered Inertial (ECI) frame

$$\overline{F} + m\overline{g}^{I} = m\frac{d}{dt}\overline{U}^{I} \tag{1}$$

where $\overline{F}$ is the sum of the aerodynamic and thrust forces, $\overline{g}^{I}$ is the gravitational acceleration observed in ECI frame, *m* is the mass of the projectile and $\overline{U}^{I}$ is the inertial velocity of the center of mass of the projectile. Note that the thrust forces must account for the mass variation of the system.

Euler's second law gives the rotational equation of motion of the projectile with respect to ECI frame

$$\overline{M} = \frac{d}{dt}\left(\underline{\mathrm{I}}\,\overline{\varpi}\right) \tag{2}$$

where $\overline{M}$ is the sum of the aerodynamic, thrust and jet damping moments referred to the center of mass of the projectile, $\underline{\mathrm{I}}$ is the matrix of inertia of the projectile referred to the center of mass and $\overline{\varpi}$ is the inertial angular velocity of the projectile.

The left side of equations (1) and (2) are said to describe the dynamics and the right side the kinematics. These are vector equations. They can be each expressed as three scalar equations for a total of six equations in six unknowns. Hence there are six degrees of freedom. The possible seventh degree of freedom will be discussed below.

The velocity of the projectile's center of mass with respect to the Earth-Centered Earth-Fixed (ECEF) frame is denoted by $\overline{U}$ and is given by

$$\overline{U} = \overline{U}^{I} - \overline{\Omega}_{\mathrm{E}} \times \overline{X} \tag{3}$$

where $\overline{\Omega}_{\mathrm{E}}$ is the angular velocity of the Earth with respect to ECI frame and $\overline{X}$ is the position of the projectile's center of mass in ECEF frame. Using equations (1) and (3), the translational equation of motion is expressed in ECEF frame by

$$\bar{F} + m\bar{A}_{C} + m\bar{g}(h,\lambda) = m\frac{d\bar{U}}{dt}$$

where $\bar{A}_{C}$ is the Coriolis acceleration and $\bar{g}(h,\lambda)$ is the acceleration of gravity observed in ECEF frame (including both the gravitational acceleration and the centrifugal acceleration due to the Earth's rotation).

It is convenient to perform the integration of the motion in a body-fixed, zero-roll or zero-spin frame. The zero-roll/-spin frames have the same pitch and yaw motion as the body-fixed frame.

Finally, the translational and rotational equations expressed in a rotating coordinate frame with an angular rate $\bar{\Omega}$ are

$$\bar{F} + m\bar{A}_{C} + m\bar{g}(h,\lambda) = m\frac{d\bar{U}}{dt} + m\bar{\Omega}\times\bar{U} \tag{4}$$

and

$$\bar{M} = \frac{d}{dt}\left(\underline{I}\,\bar{\varpi}\right) + \bar{\Omega}\times\left(\underline{I}\,\bar{\varpi}\right) \tag{5}$$

where the matrix of inertia is defined as

$$\underline{I} = \begin{bmatrix} I_{x} & -I_{xy} & -I_{xz} \\ -I_{xy} & I_{y} & -I_{yz} \\ -I_{xz} & -I_{yz} & I_{z} \end{bmatrix} \tag{6}$$

The angular velocity of the projectile is denoted by $\bar{\varpi} = (p,q,r)^{T}$ and the angular velocity of the rotating coordinate frame is denoted by $\bar{\Omega} = (\Omega_{x},q,r)^{T}$. The second and third components for the coordinate frame and the second and third components for the projectile are equal for body-fixed, zero-roll and zero-spin coordinates since all frames have the same pitch and yaw motion. Thus there is no need for the notation to distinguish between them. However, while the first components of both $\overline{\omega}$ and $\overline{\Omega}$ are identical by definition for body-fixed coordinates, the first component of $\overline{\Omega}$ will be: 0 for zero-spin coordinates and –*r* tanθ for zero-roll coordinates where θ is the projectile Euler pitch angle. Hence we denote the first component of $\overline{\Omega}$ by Ω_x so it can be specialized to the following values: *p*, 0 or –*r* tanθ. Note that $\overline{A}_C$ and $\overline{g}$ must be rotated from the ECEF frame to the integration frame. In the body-fixed frame, $\overline{A}_C$ and $\overline{g}$ are rotating. This rotation rate can be considerable for spin-stabilized projectiles. Zero-roll/-spin coordinates can circumvent this.

The treatment of the equations of motion is made specific to the projectile by supplying the physical properties, e.g., inertia data, aerodynamic coefficients, and initial conditions. The position of the gun and target are given in terms of longitude, latitude and altitude above mean sea level in the ECEF system. The meteorological data are also provided in this system. The gun quadrant elevation and azimuth are provided in the geodetic or North-East-Down (NED) system. See Annex A. The initial roll angle of the projectile in the gun is required, as are the initial *p*, *q* and *r*. For rifled barrels, *p* could also be computed from the rifling twist and muzzle velocity. The rotations between these systems are described in Annex A. The initial Euler angles can be used to obtain the initial rotation matrix and the initial conditions on the quaternion parameters can be obtained from the rotation matrix using the methods in Annex A.

4.2.2.2 <u>Equations of Motion in Body System</u>

For a 6 DOF simulation, the equations of motion consist of four blocks of vector-matrix equations based on the following vectors:

- $\overline{X}$ = position of the center of mass given in the ECEF system
- $\overline{\lambda}$ = quaternion defining the angular position of the body frame (body fixed or zero-roll/-spin frame)
- $\overline{U}$ = translational velocity of the center of mass given in the body system
- $\overline{\omega} = (p, q, r)^{\mathrm{T}}$ = angular velocity of the projectile given in the body system

While $\overline{\Omega} = (\Omega_x, q, r)^{\mathrm{T}}$ is the angular velocity of the body frame given in the body system. Ω_x can be specialized to the following values: *p* (body-fixed frame), 0 (zero-spin frame) or –*r* tanθ (zero-roll frame). See Annex A, section 1.3.

4.2.2.2.1 <u>Translational Kinematics</u>

The translational velocity of the center of mass is computed using the transformation matrix, $\underline{T}^{E/R}$, from system R (attached to the body frame) to system E (attached to the ECEF frame), as described in Annex A.

$$\frac{d\overline{X}}{dt} = \begin{bmatrix} \dot{X}_1 \\ \dot{X}_2 \\ \dot{X}_3 \end{bmatrix} = \underline{T}^{E/R}\,\overline{U} \qquad (7)$$

4.2.2.2.2 Rotational Kinematics

The quaternion parameters are propagated by the following equation of motion

$$\frac{d\overline{\lambda}}{dt} = \begin{bmatrix} \dot{\lambda}_0 \\ \dot{\lambda}_1 \\ \dot{\lambda}_2 \\ \dot{\lambda}_3 \end{bmatrix} = \frac{1}{2}\begin{bmatrix} -\lambda_1 & -\lambda_2 & -\lambda_3 \\ \lambda_0 & -\lambda_3 & \lambda_2 \\ \lambda_3 & \lambda_0 & -\lambda_1 \\ -\lambda_2 & \lambda_1 & \lambda_0 \end{bmatrix}\overline{\Omega} \qquad (8)$$

4.2.2.2.3 Translational Dynamics

The acceleration of the center of mass is given in the body fixed system as follows

$$\frac{d\overline{U}}{dt} = \begin{bmatrix} \dot{U}_x \\ \dot{U}_y \\ \dot{U}_z \end{bmatrix} = \frac{\overline{F}}{m} + \overline{g}(h,\lambda) + \overline{A}_C - \overline{\Omega}\times\overline{U} = \begin{bmatrix} F_x/m + g_x + A_x - qU_z + rU_y \\ F_y/m + g_y + A_y - rU_x + \Omega_x U_z \\ F_z/m + g_z + A_z - \Omega_x U_y + qU_x \end{bmatrix} \qquad (9)$$

See Annex A for the discussion about the Coriolis acceleration components (A_x, A_y, A_z) and gravity acceleration components (g_x, g_y, g_z). Note that the components g_x, g_y and g_z are the combined action of gravitation and the centrifugal acceleration due to the rotation of the Earth.

The applied forces F_X, F_Y and F_Z are the sum of aerodynamic and thrust forces and are defined in Annexes B, D and E.

4.2.2.2.4 Rotational Dynamics

The acceleration of the angular rate of the body is given in the body-fixed system by

$$\frac{d\overline{\omega}}{dt} = \begin{bmatrix} \dot{p} \\ \dot{q} \\ \dot{r} \end{bmatrix} = \underline{I}^{-1}\left(\overline{M} - \overline{\Omega} \times \underline{I}\,\overline{\omega} - \frac{d\,\underline{I}}{dt}\,\overline{\omega} \right) \tag{10}$$

where

$$\overline{M} - \overline{\Omega} \times \underline{I}\,\overline{\omega} = \begin{bmatrix} L \\ M \\ N \end{bmatrix} - \begin{bmatrix} qr(I_z - I_y) + prI_{xy} - pqI_{xz} + (r^2 - q^2)I_{yz} \\ prI_x - \Omega_x rI_z - qrI_{xy} + (\Omega_x p - r^2)I_{xz} + \Omega_x qI_{yz} \\ \Omega_x qI_y - pqI_x + (q^2 - \Omega_x p)I_{xy} + qrI_{xz} - \Omega_x rI_{yz} \end{bmatrix} \tag{11}$$

L, *M* and *N* are the components of the total applied moment about x, y and z axes respectively from aerodynamics and reaction forces acting about the center of mass.

A correction can be made to the applied moments for shift $\overline{\Delta} = (\Delta X, \Delta Y, \Delta Z)^{T}$ in the center of mass. Looking forward from the rear, these component shifts are positive forward, rightward, and downward respectively.

$$\overline{M}' = \begin{bmatrix} L' \\ M' \\ N' \end{bmatrix} = \overline{M} + \overline{F} \times \overline{\Delta} \tag{12}$$

Jet damping effects for a single nozzle rocket placed on the projectile symmetry axis are modeled as described in STANAG 4355.

4.2.2.3 7th Degree of Freedom – Body-fixed System

The seven degrees of freedom trajectory model is limited to dual-spin projectiles which consist of two rigid bodies that are coaxial in pitch and yaw (i.e. coaxial about the x-axis). The seventh degree of freedom is defined here as the roll position of an additional body - called body 2 - with respect to the main body.

The equation of motion of the center of mass is the same as eq. (9) for the 6 DOF body. The equation of the angular motion requires distinguishing between the angular velocities of the two bodies: p is the spin of the main body and p_2 is the spin of body 2. In general, $p \neq p_2$ but the pitch and yaw rates (q and r) are the same for both bodies. Therefore, the angular velocity vector of body 2 expressed in the main body system is

$$\bar{\omega}_2 = \begin{bmatrix} p_2 \\ q \\ r \end{bmatrix} \tag{13}$$

The quaternion defining the angular position of body 2 with respect to the main body is defined as $\bar{\mu} = (\mu_0 \quad \mu_1 \quad 0 \quad 0)^{\mathrm{T}}$. The evolution of this quaternion is an additional rotational kinematics equation defined as follows (see eq. (8))

$$\frac{d\,\bar{\mu}}{dt} = \frac{1}{2}\begin{bmatrix} -\mu_1 & 0 & 0 \\ \mu_0 & 0 & 0 \\ 0 & \mu_0 & -\mu_1 \\ 0 & \mu_1 & \mu_0 \end{bmatrix}\begin{bmatrix} p_2 - \Omega_{\mathrm{x}} \\ 0 \\ 0 \end{bmatrix} \tag{14}$$

Where Ω_{x} is the spin of the main body frame (i.e. the body-fixed, zero-roll or zero-spin frame attached to the main body).

Body 2 is supposed to be rotationally symmetric about the x-axis. Therefore, with respect to the main body frame, the inertia matrix of body 2 is diagonal and its time derivative is zero. Denoting the axial moment of inertia of body 2 by $I_{2\mathrm{x}}$, the inertia matrix of the complete projectile referred to the center of mass can be defined by the following sum

$$\underline{\mathrm{I}} + \underline{\mathrm{I}_2} = \begin{bmatrix} I_{\mathrm{x}} & -I_{\mathrm{xy}} & -I_{\mathrm{xz}} \\ -I_{\mathrm{xy}} & I_{\mathrm{y}} & -I_{\mathrm{yz}} \\ -I_{\mathrm{xz}} & -I_{\mathrm{yz}} & I_{\mathrm{z}} \end{bmatrix} + \begin{bmatrix} I_{2\mathrm{x}} & 0 & 0 \\ 0 & 0 & 0 \\ 0 & 0 & 0 \end{bmatrix} \tag{15}$$

The $\underline{\mathrm{I}}$ matrix in eq. (15) takes into account the axial inertia of the main body and the transverse inertia of the complete projectile since the two bodies pitch and yaw as a single entity.

The internal moment exerted by the main body on body 2 at the contact point *C* is to be considered. This moment may be due to bearing frictions or to some on-board control mechanism. Since the two bodies are coaxial in pitch and yaw, only the rolling component of this moment is to be considered

$$\bar{M}_C = \begin{bmatrix} L_C \\ 0 \\ 0 \end{bmatrix} \tag{16}$$

The same goes for the external moment applied to body 2

$$\overline{M}_2 = \begin{bmatrix} L_2 \\ 0 \\ 0 \end{bmatrix} \quad (17)$$

Using the notations defined in the 6 DOF section and those introduced above, the equations of the angular motion of the two bodies are then defined in the main body system as follows

$$\frac{d\overline{\omega}}{dt} = \underline{I}^{-1}\left(\overline{M} - \overline{M}_2 - \overline{M}_C - \overline{\Omega}\times\left(\underline{I}\,\overline{\omega} + \underline{I}_2\,\overline{\omega}_2\right)\right) \quad (18)$$

$$\dot{p}_2 = \frac{1}{I_{2x}}\left(L_2 + L_C\right) \quad (19)$$

4.2.2.4 Numerical Integration

The equations of motion described in sections II-2.2 and II-2.3 are all expressed in state variable form as $\dot{s} = f(s,t)$ where *s* denotes the state. Consequently, they can readily be integrated using a numerical method such as the Runge-Kutta algorithm discussed in Annex G.

4.2.3 Atmospheric Modeling

This 6/7 DOF guided projectile simulation uses the standard atmospheric model used for the modified point-mass model in STANAG 4355. It will be compatible with any new STANAG regarding atmospheric modeling such as the multi-dimensional model and is be consistent with standard met messages. See STANAG 6022.

4.3 List Of Symbols

Symbol	Definition	Unit
$\overline{A}_C$	Coriolis acceleration vector.	m/s^2
A_x, A_y, A_z	Components of the Coriolis acceleration in EOM (body-fixed or zero-roll/-spin) coordinates.	m/s^2
$\overline{F}$	Vector sum of applied forces acting on projectile center of mass.	N
F_x, F_y, F_z	Components of total applied forces (aerodynamic, thrust) in EOM (body-fixed or zero-roll/-spin) coordinates.	N
$\overline{g}(h,\lambda)$	Acceleration of gravity at projectile position with respect to ECEF frame. It includes the combined action of gravitation and the centrifugal acceleration due to the rotation of the Earth. See Annex A.	m/s^2
g_x, g_y, g_z	Components of $\overline{g}(h,\lambda)$ in EOM (body-fixed or zero-roll/-spin) coordinates.	m/s^2
$\underline{I}$	Inertia tensor of the projectile rigid body.	$kg\,m^2$
I_{xy}, I_{xz}, I_{yz}	Products of inertia with respect to the coordinate planes.	$kg\,m^2$
I_{1x}, I_{2x}	Axial moments of inertia of bodies 1 and 2 in 7th degree of freedom mode.	$kg\,m^2$
L, M, N	Components of total applied moment or torque.	$N\,m$
L', M', N'	Components of total applied moment or torque corrected for the change in position of the center of mass.	$N\,m$
L_2	Axial component of external moment applied on body 2 in 7th degree of freedom mode.	$N\,m$
L_C	Axial component of the internal moment exerted by body 1 on body 2 in 7th degree of freedom mode (depends on bearing friction and controls).	$N\,m$

$\overline{M}$	Total applied moment or torque acting on projectile with respect to center of mass.	*N m*
$\overline{M}'$	Total applied moment or torque acting on projectile corrected for the change $\overline{\varDelta}$ in position of the center of mass.	*N m*
$\overline{M}_2$	External moment applied to body 2 in 7^{th} degree of freedom mode.	*N m*
$\overline{M}_C$	Internal moment exerted by body 1 on body 2 at contact point *C* in 7^{th} degree of freedom mode.	*N m*
m	Total mass of the projectile.	*kg*
p, *q* , *r*	Components of the angular velocity of the projectile in EOM (body-fixed or zero-roll/-spin) coordinates.	*rad/s*
p_1 , p_2	Axial component of the angular velocity of bodies 1 and 2 in 7^{th} degree of freedom mode.	*rad/s*
t	Time.	*s*
$\overline{U}$	Velocity of the projectile center of mass with respect to ECEF frame.	*m/s*
U_x, U_y, U_z	Components of $\overline{U}$ in EOM (body-fixed or zero-roll/-spin) coordinates.	*m/s*
u	Speed of the projectile center of mass with respect to ECEF frame (ground speed).	*m/s*
$\overline{X}$	Position of the projectile center of mass with respect to ECEF frame.	*m*
$\overline{\varDelta}$	Vector shift in the center of mass.	*m*
λ	Latitude of the fire control system.	*deg*

$\bar{\lambda}$	Quaternion defining the angular position of the projectile (EOM system) with respect to inertial system. See Annex A.	-
$\lambda_0, \lambda_1, \lambda_2, \lambda_3$	Components of quaternion $\bar{\lambda}$. See Annex A.	-
$\bar{\mu}$	Quaternion defining the angular position of body 2 with respect to body 1 in 7th degree of freedom mode.	-
μ_0, μ_1	Components of quaternion $\bar{\mu}$.	-
θ	Pitch angle of the projectile.	*rad*
$\bar{\Omega}$	Angular velocity vector of the body integration (EOM) frame with respect to ECI frame. The x, y, z components are called Ω_X , *q* and *r* in EOM (body-fixed or zero-roll/-spin) coordinates.	*rad/s*
$\bar{\Omega}_E$	Angular velocity vector of the Earth with respect to ECI frame.	*rad/s*
$\bar{\varpi}$	Angular velocity vector of the projectile with respect to ECI frame. The x, y, and z components are conventionally called *p*, *q* and *r* in EOM (body-fixed or zero-roll/-spin) coordinates.	*rad/s*
$\bar{\varpi}_1, \bar{\varpi}_2$	Angular velocity vectors of bodies 1 and 2 in 7th degree of freedom mode.	*rad/s*
•	Denotes differentiation with respect to time.	s^{-1}

4.4 LIST OF DATA REQUIREMENTS

Physical Data Requirements	***Fin-Stabilized***	***Spin-Stabilized***
Twist of rifling at muzzle	t_c	t_c
Total mass of projectile	m	m
Reference diameter	d	d
Axial moment of inertia	I_x	I_x
Axial moment of inertia of body 2 (7th DOF)	I_{2x}	I_{2x}
Initial axial spin rate of projectile body	p_0	p_0
Initial axial spin rate of body 2 (7th DOF)	p_{2_0}	p_{2_0}
Axial torque between two bodies at contact point (7th DOF)	L_C	L_C
Transverse moment of inertia (x-axis symmetry)		I_T
Transverse moment of inertia about Y	I_Y	
Transverse moment of inertia about Z	I_Z	
Center of mass (CG) from nose	X_{CG}	X_{CG}
X component of CG shift	ΔX	ΔX
Y component of CG shift	ΔY	ΔY
Z component of CG shift	ΔZ	ΔZ

Aerodynamic Requirements	***Fin-Stabilized***	***Spin-Stabilized***
Axial force coefficient	C_X	C_X
Normal force coefficient	C_N	C_N
Side force coefficient	C_Y	
Magnus force coefficient	C_{Yp}	C_{Yp}
Pitching (overturning) moment coefficient	C_m	C_m
Yawing moment coefficient	C_n	
Magnus moment coefficient	C_{np}	C_{np}
Roll moment coefficient	C_l	C_l
Pitch damping	C_{mq}	C_{mq}
Yaw damping	C_{mr}	C_{mr}
Roll damping moment coefficient	C_{lp}	C_{lp}
Axial force coefficient increment	ΔC_X	
Normal force coefficient increment	ΔC_N	
Side force coefficient increment	ΔC_Y	
Pitching (overturning) moment coefficient increment	ΔC_m	

Yawing moment coefficient increment	ΔC_n	
Roll moment coefficient increment	ΔC_l	

Factors for adjusting data	***Fin-Stabilized***	***Spin-Stabilized***
Form factor for axial force coefficient	f_{CX}	f_{CX}
Form factor for normal force coefficient	f_{CN}	f_{CN}
Form factor for side force coefficient	f_{CY}	
Form factor for Magnus force coefficient		f_{CYp}
Form factor for pitching moment coefficient	f_{Cm}	f_{Cm}
Form factor for yawing moment coefficient	f_{Cn}	
Form factor for Magnus moment coefficient		f_{Cnp}
Form factor for roll moment coefficient	f_{Cl}	f_{Cl}
Form factor for pitch damping	f_{Cmq}	f_{Cmq}
Form factor for yaw damping	f_{Cmr}	f_{Cmr}
Form factor for roll damping coefficient	f_{Clp}	f_{Clp}
Form factor for axial force increment coefficient	f_{CX_D}	
Form factor for normal force increment	f_{CN_D}	
Form factor for side force increment	f_{CY_D}	
Form factor for pitching moment increment coefficient	f_{Cm_D}	
Form factor for yawing moment increment	f_{Cn_D}	
Form factor for roll moment increment	f_{Cl_D}	

Form factors are scaling factors for the aerodynamic coefficients.

Initial Conditions	***Fin-Stabilized***	***Spin-Stabilized***
Initial speed of projectile with respect to ground (muzzle velocity)	u_0	u_0
Quadrant elevation	QE	QE
Azimuth with respect to true north	Az	Az
Longitude	Λ	Λ
Geodetic latitude	λ	λ
Altitude above average sea level (WGS-84 model)	h_M	h_M

Azimuth angles range from 0° (north) to 360° (north), through 90° (east), 180° (south), 270° (west).

5 IMPLEMENTATION OF THE AGREEMENT

This STANREC is implemented when a nation has issued instructions to the agencies concerned to use the 6/7 Degrees of Freedom Trajectory Model for exterior ballistics simulation of artillery projectiles as detailed in this agreement**.**

The source code will be treated as NATO Restricted and the executable will be treated as NATO Unclassified.

INTENTIONALLY BLANK

ANNEX A COORDINATE TRANSFORMATIONS, REFERENCE COORDINATE SYSTEMS AND ELLIPSOIDAL EARTH MODEL

1. Coordinate Transformations, Euler Angles And Quaternions

Frames and coordinate systems are to be distinguished. Frames are models of physical references, whereas coordinate systems establish the association with Euclidean space (see reference [14] in Annex H). Frames are set of points attached to physical objects such as the Earth or the projectile body. They are used to define the relative state of motion (position and velocity) of these objects. Each frame can be associated to several coordinate systems in order to describe the observation of the motion. Coordinate systems define the metric of the motion.

1.1 Consider two orthogonal right-handed coordinate systems denoted as $A(1^A, 2^A, 3^A)$ and $B(1^B, 2^B, 3^B)$. Let $[x]^A$ be the components of vector $\bar{x}$ in system *A* and let $[x]^B$ be the components of the same vector in system *B*. The transformation matrix $[T]^{B/A}$ from system *A* to system *B* is defined by

$$[x]^B = [T]^{B/A}[x]^A \tag{A.1}$$

The matrix $[T]^{B/A}$ transforms the components of a vector expressed in system *A* to the vector's components expressed in system *B*. The inverse transformation is denoted by $[T]^{A/B}$.

The only transformations that will be considered hereafter are orthogonal rotations. If $[T]^{B/A}$ is an orthogonal rotation matrix then

$$\det([T]^{B/A}) = 1 \tag{A.2}$$

$$([T]^{B/A})^{-1} = [\bar{T}]^{B/A} \tag{A.3}$$

Orthogonal matrices preserve length, i.e. the norm of any vector they multiply is preserved.

1.2 The matrix [*T*] used to rotate the components of a vector from one coordinate system to another may be obtained either from Euler angles or from the quaternion parameters. The 6/7 DOF simulation will use Euler angles for input and output for convenience. But internally, the 6/7 DOF simulation uses a quaternion representation because of computational efficiency and to avoid singularities associated with Euler angles.

The rotation from the non-rotating inertial axes (coordinate system *I* associated to the inertial frame) to the rotating body-fixed axes (coordinate system *B* associated to the body-fixed frame) is represented using the standard aerospace Euler rotation sequence: a yaw (angle ψ) followed by a pitch (angle θ) followed by a roll (angle ϕ).

Figure A.1 shows the yaw rotation that takes system $I(1^I, 2^I, 3^I)$ to the first intermediate system $X(1^X, 2^X, 3^X)$ through a positive rotation of angle ψ about the 3-axis. The yaw rotation matrix is defined by

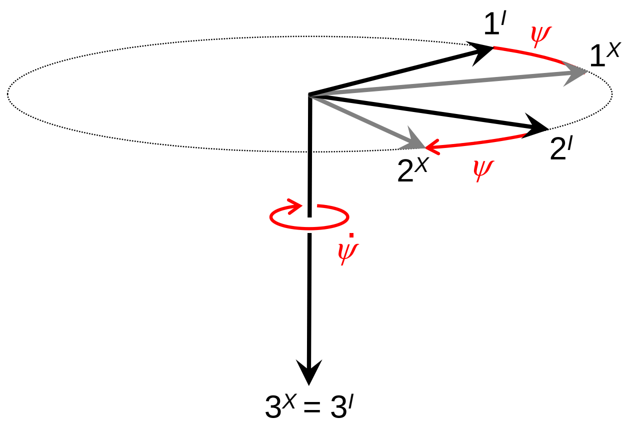

$$[T(\psi)] = [T]^{X/I} = \begin{bmatrix} \cos\psi & \sin\psi & 0 \\ -\sin\psi & \cos\psi & 0 \\ 0 & 0 & 1 \end{bmatrix} \tag{A.4}$$

Figure A.1: Yaw rotation

Figure A.2 shows the pitch rotation that takes system $X(1^X, 2^X, 3^X)$ to the second intermediate system $Y(1^Y, 2^Y, 3^Y)$ through a positive rotation of angle θ about the 2-axis. The pitch rotation matrix is defined by

$$[T(\theta)] = [T]^{Y/X} = \begin{bmatrix} \cos\theta & 0 & -\sin\theta \\ 0 & 1 & 0 \\ \sin\theta & 0 & \cos\theta \end{bmatrix} \tag{A.5}$$

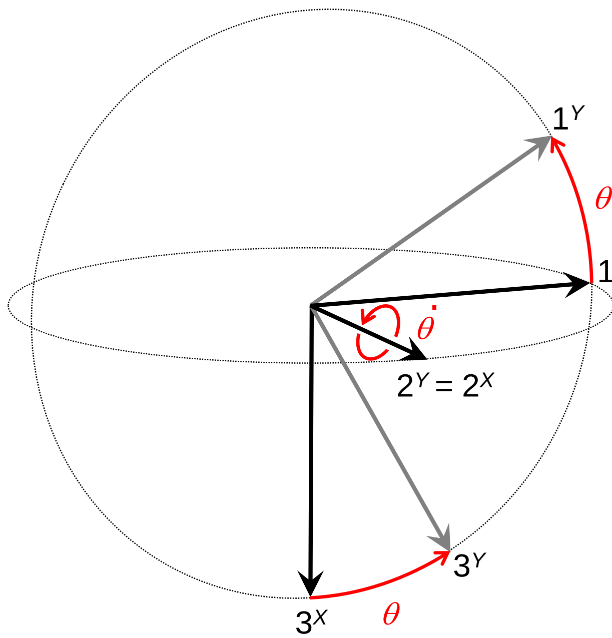

Figure A.2: Pitch rotation

Figure A.3 shows the roll rotation that takes system $Y(1^Y, 2^Y, 3^Y)$ to the body-fixed system $B(1^B, 2^B, 3^B)$ through a positive rotation of angle ϕ about the 1-axis. The roll rotation matrix is defined by

$$[T(\phi)] = [T]^{B/Y} = \begin{bmatrix} 1 & 0 & 0 \\ 0 & \cos\phi & \sin\phi \\ 0 & -\sin\phi & \cos\phi \end{bmatrix} \tag{A.6}$$

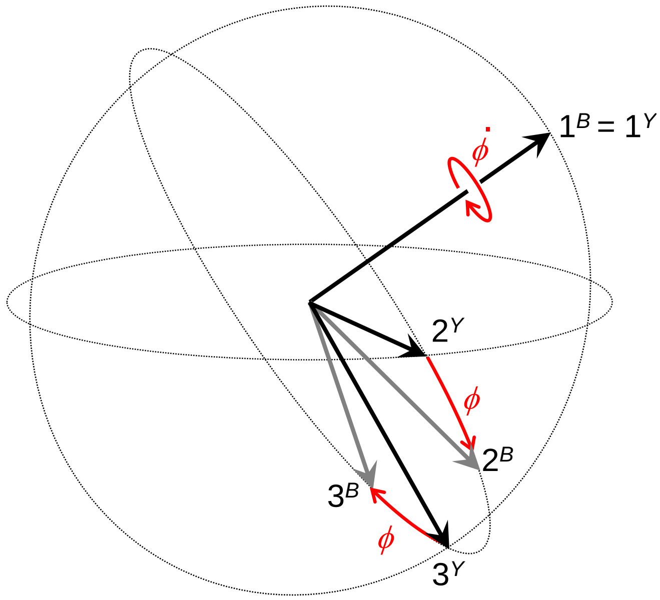

Figure A.3: Roll rotation

The total rotation matrix that gives in the body-fixed system *B* the components of a vector defined in the inertial system *I* is the product of the three Euler rotation matrices:

$$[T]^{B/I} = [T]^{B/Y}[T]^{Y/X}[T]^{X/I} = [T(\phi)][T(\theta)][T(\psi)] \quad \text{(A.7)}$$

Multiplying out (A.7) yields

$$[T]^{B/I} = \begin{bmatrix} \cos\psi\cos\theta & \sin\psi\cos\theta & -\sin\theta \\ -\sin\psi\cos\phi + \cos\psi\sin\theta\sin\phi & \cos\psi\cos\phi + \sin\psi\sin\theta\sin\phi & \cos\theta\sin\phi \\ \sin\psi\sin\phi + \cos\psi\sin\theta\cos\phi & -\cos\psi\sin\phi + \sin\psi\sin\theta\cos\phi & \cos\theta\cos\phi \end{bmatrix} \quad \text{(A.8)}$$

1.3 Let $[\omega^{B/I}]$ be the angular velocity vector related to the rotation matrix $[T]^{B/I}$. This vector is defined in the body-fixed system by

$$[\omega^{B/I}]^B = \begin{bmatrix} p \\ q \\ r \end{bmatrix} = \begin{bmatrix} \dot\phi - \dot\psi\sin\theta \\ \dot\theta\cos\phi + \dot\psi\sin\phi\cos\theta \\ -\dot\theta\sin\phi + \dot\psi\cos\phi\cos\theta \end{bmatrix} \quad \text{(A.9)}$$

Eq. (A.9) cannot be inverted for $\theta = \pm\pi/2$. The Euler angle representation suffers from singularities at vertical climb and dive.

The zero-roll coordinate system is derived from the body-fixed system by setting $\phi = 0$ and $\dot\phi = 0$. The angular velocity of the zero-roll system is thus defined by

$$[\omega^{ZR/I}]^{ZR} = \begin{bmatrix} -\dot\psi\sin\theta \\ \dot\theta \\ \dot\psi\cos\theta \end{bmatrix} = \begin{bmatrix} -r\tan\theta \\ q \\ r \end{bmatrix} \quad \text{(A.10)}$$

Note that *q* and *r* are the second and third coordinates of $[\omega^{B/I}]$ given in the zero-roll system. The zero-roll coordinate system cannot be defined using *q* and *r* for $\theta = \pm\pi/2$.

The zero-spin coordinate system is derived from the body-fixed system by setting $\dot\phi = \dot\psi\sin\theta$. The angular velocity of the zero-spin system is thus defined by

$$[\omega^{ZS/I}]^{ZS} = \begin{bmatrix} 0 \\ q \\ r \end{bmatrix} \quad \text{(A.11)}$$

Note that *q* and *r* are the second and third coordinates of $[\omega^{B/I}]$ given in the zero-spin system.

When using a zero-spin system, the roll Euler angle of the projectile is defined by

$$\phi_{\mathrm{B}} = \phi_{\mathrm{ZP}} + \int p\,dt + \phi_0 \qquad \text{(A.12)}$$

where ϕ_{B} is the projectile roll angle in body-fixed coordinates, ϕ_{ZP} is the projectile roll angle in zero-spin coordinates, p is the spin rate of the projectile and ϕ_0 is the initial projectile roll angle.

1.4 There are many ways to choose to define the Euler angles. But no matter the choice, there is always a singularity is some direction. Singularities can be avoided completely by using the four quaternion parameters with body-fixed or zero-spin coordinates. The 6/7 DOF code will use the quaternion parameters internally to avoid the singularity for body-fixed and zero-spin systems and also because they are computationally faster since they avoid the evaluation of trigonometric functions. The Euler angles will be used for input and output because of their familiarity.

1.5 The matrix $[T]^{B/I}$ may also be computed from the unit quaternion. The quaternion is a set of four parameters $\lambda_0, \lambda_1, \lambda_2$ and λ_3. A unit quaternion is normalized, i.e. $\lambda_0^2 + \lambda_1^2 + \lambda_2^2 + \lambda_3^2 = 1$. The parameter λ_0 is called the "scalar part" and the triplet λ_1, λ_2 and λ_3 is called the "vector part". The quaternion was originally defined as the generalization of a complex number and could be written $\lambda_0 + \mathrm{i}\lambda_1 + \mathrm{j}\lambda_2 + \mathrm{k}\lambda_3$ where $\mathrm{i}^2 = \mathrm{j}^2 = \mathrm{k}^2 = -1$ and ij = k, jk = i, ki = j and i, j and k anti-commute. The properties of quaternions can be derived from these definitions. There is also a physical interpretation. Any rotation, even if it is composed of several sub-rotations such as roll, pitch and yaw about different intermediate axes can also be realized by a single rotation through a single angle about a single axes. It can be shown that the 'vector part' of a quaternion is the axis of that rotation and the 'scalar part' is a trigonometric function of the rotation angle. Specifically the rotation angle is $\theta = 2\cos^{-1}\lambda_0$ and the axis of rotation is $\bar{\mathrm{n}} = \lambda_1\bar{\mathrm{i}} + \lambda_2\bar{\mathrm{j}} + \lambda_3\bar{\mathrm{k}}$ where here $\bar{\mathrm{i}}, \bar{\mathrm{j}}$ and $\bar{\mathrm{k}}$ denote the unit vectors along *x*, *y* and *z*.

Using the quaternion parameters, the rotation matrix that gives in the body-fixed system *B* the components of a vector defined in the inertial system *I* is

$$[T]^{B/I} = \begin{bmatrix} \lambda_0^2+\lambda_1^2-\lambda_2^2-\lambda_3^2 & 2(\lambda_1\lambda_2+\lambda_0\lambda_3) & 2(\lambda_1\lambda_3-\lambda_0\lambda_2) \\ 2(\lambda_1\lambda_2-\lambda_0\lambda_3) & \lambda_0^2-\lambda_1^2+\lambda_2^2-\lambda_3^2 & 2(\lambda_2\lambda_3+\lambda_0\lambda_1) \\ 2(\lambda_1\lambda_3+\lambda_0\lambda_2) & 2(\lambda_2\lambda_3-\lambda_0\lambda_1) & \lambda_0^2-\lambda_1^2-\lambda_2^2+\lambda_3^2 \end{bmatrix} \qquad \text{(A.13)}$$

<u>1.5</u> Method for transforming between Euler angles and quaternions using matrix $[T]^{B/I}$

As indicated above, a quaternion is used internally in the simulation, with inputs and outputs expressed in Euler angles. Thus there is a requirement to transform from the Euler angles to the equivalent quaternion and vice versa. The algorithm proceeds as follows. Obtain the rotation matrix $[T]^{B/I}$. The rotation matrix is numerically the same whether it is obtained from the Euler angles or the quaternion. Once the rotation matrix is obtained from either the Euler angles or from the quaternion, it is then possible to reverse the process and obtain either Euler angles or quaternion from the rotation matrix.

The Euler angles can be obtained from $[T]^{B/I}$ (or directly from the quaternion parameters) with the following formulae

$$\tan\psi = \frac{T_{12}}{T_{11}} = \frac{2(\lambda_1\lambda_2+\lambda_0\lambda_3)}{\lambda_0^2+\lambda_1^2-\lambda_2^2-\lambda_3^2} \qquad -\pi < \psi \le \pi \qquad \text{(A.14)}$$

$$\sin\theta = -T_{13} = 2(\lambda_0\lambda_2-\lambda_1\lambda_3) \qquad -\pi/2 \le \theta \le \pi/2 \qquad \text{(A.15)}$$

$$\tan\phi = \frac{T_{23}}{T_{33}} = \frac{2(\lambda_2\lambda_3+\lambda_0\lambda_1)}{\lambda_0^2-\lambda_1^2-\lambda_2^2+\lambda_3^2} \qquad 0 \le \phi < 2\pi \qquad \text{(A.16)}$$

When programming the inverse tangent, a two-parameter arctangent function (such as ATAN2 function which is available in FORTRAN 90/95) must be used in order to obtain ψ and ϕ (note that the angle returned by ATAN2 is in the range $]-\pi, +\pi]$). Also, if the arctangent function is undefined if both arguments are zero, this needs to be trapped and dealt with separately.

The quaternion parameters can also be obtained from the Euler angles by first obtaining the rotation matrix $[T]^{B/I}$. See (A.8). There are four ways to obtain the results we seek from the rotation matrix elements. Define $T_{00} \equiv \mathrm{Trace}([T]^{B/I}) = \sum_{i=1}^{3} T_{\mathrm{ii}}$. Compare the four elements defined by (1 + 2Tii – T00) where i = 0, 1, 2, 3. Find which of these elements has the dominant value (i.e. the largest maximum value since these elements are all greater than or equal to zero). In case of multiple occurrences of maximum values, the dominant element can be arbitrarily chosen as the first occurrence. The quaternion with the same subscript is the dominant quaternion and the subscript is the dominant subscript. Then use one of the following 4 recipes, where the first lambda in each of the four cases has the dominant subscript. This assures that the denominator always has the largest absolute value and improves numerical calculations.

$(1+T_{00})$ is dominant (A.17)

$$\lambda_0 = \frac{1}{2}\left(1+T_{00}\right)^{1/2}$$

$$\lambda_1 = \frac{1}{4\lambda_0}\left(T_{23}-T_{32}\right)$$

$$\lambda_2 = \frac{1}{4\lambda_0}\left(T_{31}-T_{13}\right)$$

$$\lambda_3 = \frac{1}{4\lambda_0}\left(T_{12}-T_{21}\right)$$

$(1+2T_{11}-T_{00})$ is dominant (A.18)

$$\lambda_1 = \frac{1}{2}\left(1+2T_{11}-T_{00}\right)^{1/2}$$

$$\lambda_0 = \frac{1}{4\lambda_1}\left(T_{23}-T_{32}\right)$$

$$\lambda_2 = \frac{1}{4\lambda_1}\left(T_{12}+T_{21}\right)$$

$$\lambda_3 = \frac{1}{4\lambda_1}\left(T_{13}+T_{31}\right)$$

$(1+2T_{22}-T_{00})$ is dominant (A.19)

$$\lambda_2 = \frac{1}{2}\left(1+2T_{22}-T_{00}\right)^{1/2}$$

$$\lambda_0 = \frac{1}{4\lambda_2}\left(T_{31}-T_{13}\right)$$

$$\lambda_1 = \frac{1}{4\lambda_2}\left(T_{12}+T_{21}\right)$$

$$\lambda_3 = \frac{1}{4\lambda_2}\left(T_{23}+T_{32}\right)$$

$(1+2T_{33}-T_{00})$ is dominant (A.20)

$$\lambda_3 = \frac{1}{2}\left(1+2T_{33}-T_{00}\right)^{1/2}$$

$$\lambda_0 = \frac{1}{4\lambda_3}\left(T_{12}-T_{21}\right)$$

$$\lambda_1 = \frac{1}{4\lambda_3}\left(T_{13}+T_{31}\right)$$

$$\lambda_2 = \frac{1}{4\lambda_3}\left(T_{23}+T_{32}\right)$$

1.6 Method for computing quaternions directly from Euler angles

The four parameters of the unit quaternion can be directly computed using the three Euler angles as follows:

$$\lambda_0 = \cos\frac{\psi}{2}\cos\frac{\theta}{2}\cos\frac{\phi}{2} + \sin\frac{\psi}{2}\sin\frac{\theta}{2}\sin\frac{\phi}{2} \quad \text{(A.21)}$$

$$\lambda_1 = \cos\frac{\psi}{2}\cos\frac{\theta}{2}\sin\frac{\phi}{2} - \sin\frac{\psi}{2}\sin\frac{\theta}{2}\cos\frac{\phi}{2} \quad \text{(A.22)}$$

$$\lambda_2 = \cos\frac{\psi}{2}\sin\frac{\theta}{2}\cos\frac{\phi}{2} + \sin\frac{\psi}{2}\cos\frac{\theta}{2}\sin\frac{\phi}{2} \quad \text{(A.23)}$$

$$\lambda_3 = -\cos\frac{\psi}{2}\sin\frac{\theta}{2}\sin\frac{\phi}{2} + \sin\frac{\psi}{2}\cos\frac{\theta}{2}\cos\frac{\phi}{2} \quad \text{(A.24)}$$

1.7 List of symbols

Symbol	Definition	Unit
p, q, r	Components of the angular velocity of the projectile in EOM (body-fixed or zero-roll/-spin) coordinates.	*rad/s*
$[T]^{B/I}$	Transformation matrix from system *I* to system *B*.	-
θ	Pitch Euler angle.	*rad*
λ_0	Scalar component of quaternion.	-
$\lambda_1, \lambda_2, \lambda_3$	Vector component of quaternion.	-
ϕ	Roll Euler angle.	*rad*
ϕ_{B}	Projectile roll angle in body-fixed coordinates.	*rad*
ϕ_{ZP}	Projectile roll angle in zero-spin coordinates.	*rad*
ϕ_0	Initial Projectile roll angle.	*rad*
ψ	Yaw Euler angle.	*rad*

2. Reference Coordinate Systems

ECI reference system
Non-rotating, Cartesian, Earth-centered inertial system, with Z pointing northward from the center of the Earth, X pointing toward the sun at the vernal equinox and Y completing a right hand set. The origin is at the center of the Earth. See Figure A.4.

ECEF reference system
Rotating, Cartesian, Earth-centered Earth-fixed system, with Z pointing northward from the center of the Earth, X pointing toward the Greenwich meridian and Y completing a right hand set. The origin is at the center of the Earth. See Figure A.4.

Geocentric reference system
Rotating, Cartesian, Earth-fixed system, with X northward, Z toward the center of the Earth and Y eastward completing an orthogonal right-handed set. The origin is on the surface of the Earth. See Figure A.5.

North-East-Down (NED) system
Orthogonal, right-handed coordinate system fixed to Earth. The origin can be located at any specific point (gun, target, etc). The x-axis is pointing northward (N), the y-axis is pointing eastward (E) and the z-axis is pointing downward (direction of the local gravity). Note that the NED system can also be called the local geodetic system. See Figure A.6.

Fire control system
Orthogonal, right-handed coordinate system fixed to Earth. The origin is on the surface of the Earth with x-axis (coordinate 1) in the direction of the target, y-axis (coordinate 2) pointing upward (opposite direction of the local gravity) and z-axis (coordinate 3) pointing to the right in order to complete the right hand set. See Figure 1. This system complies with STANAG 4355.

Body-fixed system
Orthogonal, right-handed coordinate system fixed to the projectile, with the origin at the center of mass, consisting of the following axes: x-axis in the reference plane (plane of symmetry if any), y-axis normal to the reference plane and positive to starboard, z-axis completing the right hand set. See Figure 1. This system complies with ISO 1151.

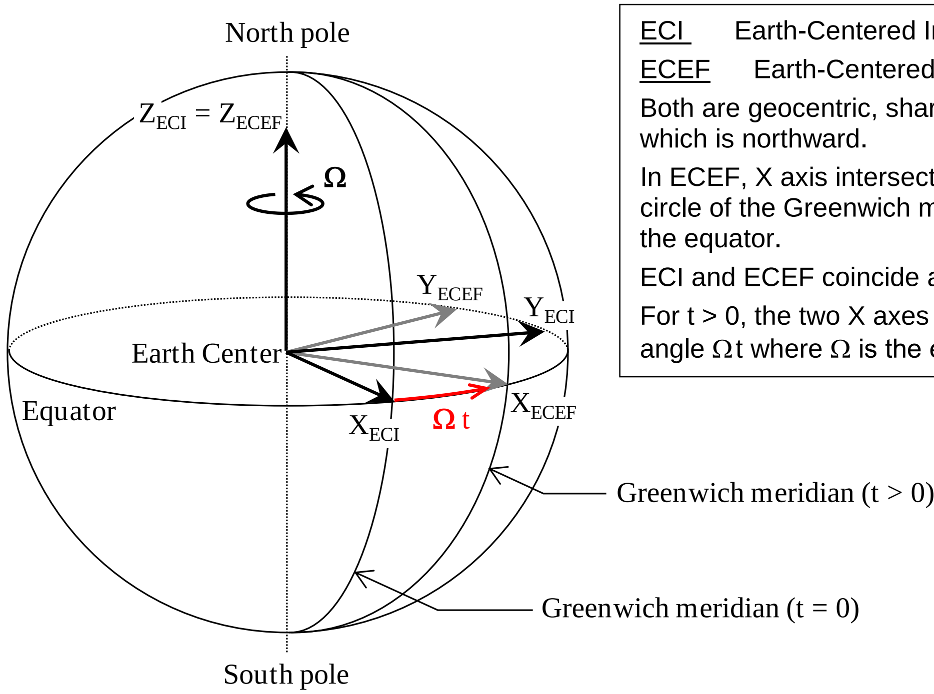

ECI Earth-Centered Inertial

ECEF Earth-Centered Earth-Fixed

Both are geocentric, share Z axis which is northward.

In ECEF, X axis intersects the great circle of the Greenwich meridian and the equator.

ECI and ECEF coincide at t = 0.

For t > 0, the two X axes differ by angle Ωt where Ω is the earth's

Figure A.4: ECI and ECEF Systems

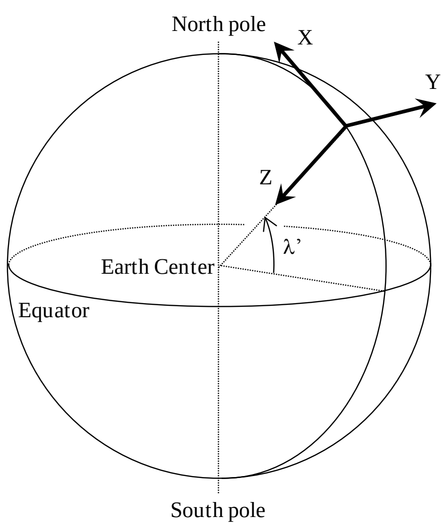

Geocentric System

Z is toward center of earth

X is northward

Y is eastward

X, Y, Z are right-handed and orthogonal

Figure A.5: Geocentric System

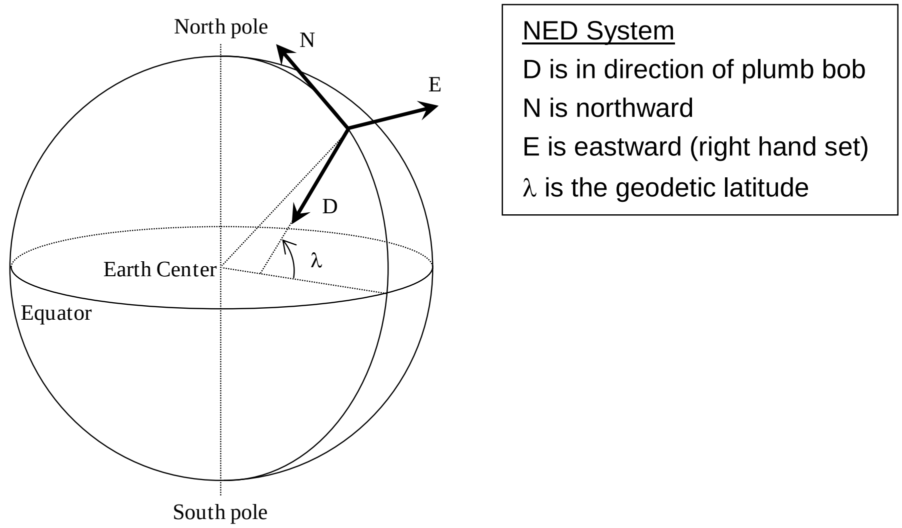

Figure A.6: NED System

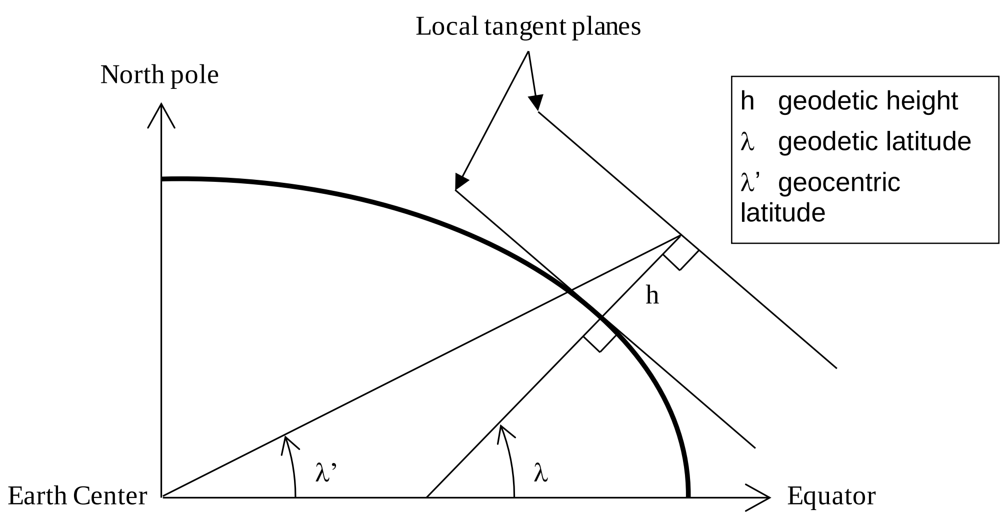

Figure A.7: Geodetic and Geocentric Latitudes

3. Ellipsoidal Earth Model

3.1 The WGS-84 (World Geodetic Survey) Ellipsoidal Earth Model is appropriate to use because of the interest in the GPS (Global Positioning System). The ellipsoidal Earth can be thought of as the shape that the Earth would take if it were entirely liquid. The surface of this ellipsoid results from the combined action of gravitation and the centrifugal acceleration due to the rotation of the Earth. The normal to the local surface is defined as "down" and is the direction of a plumb bob at that point. This "down" does not, in general, point toward the center of the Earth because of the combined effects of gravitation and the centrifugal acceleration from the Earth's rotation about its axis. The effect of the accelerations due to the revolution of the Earth about the sun is neglected.

3.2 In the trajectory or flight simulation, the treatment of gravity and atmospheric modeling will have to be consistent with model used. In our case, we will use an ECEF WGS-84 ellipsoid Earth model. Transformations of coordinates to and from the ECEF and the local navigation frame (geographic frame) will be necessary. Since this is essentially a geometric problem, the following figures will be used to define the problem and its solution. Recall that "down" is defined as the direction of a plumb bob.

3.3 Coordinate transformations between Geodetic and ECEF reference frames

We require transformations to and from the longitude Λ, geodetic latitude λ and altitude h of the projectile and the ECEF coordinates X, Y, Z (see Figure A.7). The geocentric latitude λ' is defined by the angle between a geocentric vector (one that originates at the center of the Earth) and its projection on the equatorial plane. The geodetic latitude λ is defined by the angle between the vector that is normal to the local tangent plane to the reference ellipsoid and its projection onto the equatorial plane. The altitude h is the shortest distance between the projectile and the reference ellipsoid. The equatorial and polar radii of the ellipsoidal Earth are denoted by a and b respectively. Here a transformation is required between an altitude and the longitude and latitude which are angles and the Earth-centered Earth-fixed Cartesian coordinates X, Y and Z. The altitude h is useful for atmospheric modeling.

We will need the following quantities that define the WGS-84 ellipsoidal Earth.

a is the semi-major axis of reference ellipse, equatorial radius of Earth in meters.
b is the semi-minor axis of reference ellipse, polar radius of Earth in meters.
$e=\sqrt{1-(b/a)^2}$ is the eccentricity.
$\bar{r}=(X,Y,Z)^{\mathrm{T}}$ is the ECEF position vector of projectile.

3.4 Transformation from the Geodetic to the ECEF frame: *h*, *Λ* and *λ* to *X*, *Y* and *Z*

The longitude and latitude are ordinary in degrees. Care must be taken to convert to radians when these angles are arguments of trigonometric functions.

We want to transform from the longitude *Λ*, geodetic latitude *λ,* and altitude *h* of the projectile to the ECEF coordinates *X*, *Y*, *Z*. From geometry the result is

$$\begin{bmatrix} X \\ Y \\ Z \end{bmatrix} = \begin{bmatrix} \left(h + \dfrac{a}{\sqrt{1 - e^2 u_Z^2}} \right) u_X \\ \left(h + \dfrac{a}{\sqrt{1 - e^2 u_Z^2}} \right) u_Y \\ \left(h + \dfrac{a\,(1 - e^2)}{\sqrt{1 - e^2 u_Z^2}} \right) u_Z \end{bmatrix} \tag{A.25}$$

where we define the unit vector pointing up as

$$\begin{bmatrix} u_X \\ u_Y \\ u_Z \end{bmatrix} = \begin{bmatrix} \cos\Lambda\cos\lambda \\ \sin\Lambda\cos\lambda \\ \sin\lambda \end{bmatrix} \tag{A.26}$$

Note that the radius of the Earth ellipsoid at this latitude can be obtained by taking the root sum square of (A.25) with *h* = 0, or

$$r_\lambda = \frac{a^2}{1 - e^2\, sin^2\,\lambda} \left(1 - 2e^2\, sin^2\,\lambda + e^4\, sin^4\,\lambda \right) \tag{A.27}$$

3.5 Transformation from the ECEF to the Geodetic reference frame: *X*, *Y* and *Z* to *h*, *Λ* and *λ*

The following algorithm transforms from the Cartesian ECEF coordinates *X*, *Y* and *Z* to the WGS-84 ellipsoidal coordinates longitude *Λ*, geodetic latitude *λ* and altitude *h*. This is the typical format of a GPS receiver. The longitude is defined as zero at the prime meridian (through Greenwich, England). It is conventionally positive to the east and negative to the west. The latitude is positive in the northern hemisphere (Z > 0) and negative in the southern hemisphere. The algorithm is as follows.

We define the quantity

$$\rho = \frac{a}{\sqrt{1-e^2u_Z^2}} = \frac{a}{\sqrt{u_X^2 + u_Y^2 + (1-e^2)u_Z^2}} \quad \text{(A.28)}$$

Then we can rewrite (A.25) as

$$\begin{bmatrix} u_X \\ u_Y \\ u_z \end{bmatrix} = \begin{bmatrix} \dfrac{X}{h+\rho} \\ \dfrac{Y}{h+\rho} \\ \dfrac{Z}{h+(1-e^2)\rho} \end{bmatrix} \quad \text{(A.29)}$$

Squaring (A.28) and substituting the components of (A.29) yields

$$a^2 = \frac{X^2+Y^2}{\left(\dfrac{h}{\rho}+1\right)^2} + \frac{(1-e^2)Z^2}{\left(\dfrac{h}{\rho}+1-e^2\right)^2} \quad \text{(A.30)}$$

With the assumption

$$\xi = 1+\frac{h}{\rho} \cong 1 \quad \text{(A.31)}$$

we can rewrite (A.30) as

$$\mathrm{f}(\xi) = 0 = \frac{X^2+Y^2}{\xi^2} + \frac{(1-e^2)Z^2}{(\xi-e^2)^2} - a^2 \quad \text{(A.32)}$$

This expression can be normalized by multiplying by the denominators, yielding a 4th order or biquartic polynomial algebraic equation in ξ that can be solved exactly by well-known but tedious methods. But since ξ has been assumed to be so close to unity, this polynomial lends itself to a recursive numerical solution such as Newton-Raphson. The iterative solution is

$$\xi_{n+1} = \xi_n - \frac{f(\xi)}{df(\xi)/d\xi} \tag{A.33}$$

where

$$df(\xi)/d\xi = -2\left(\frac{X^2+Y^2}{\xi^3} + \frac{(1-e^2)Z^2}{(\xi-e^2)^3}\right) \tag{A.34}$$

If the initial solution is taken to be $\xi_0 = 1$ then algorithm converges in several iterations, ξ_2 being accurate to the order of a millimeter. As the 6/7 degrees of freedom simulation runs, convergence is achieved in fewer steps by using the value of ξ from the previous integration step for ξ_0 (the 6/7 DOF simulation will check the iterations for convergence.) The solution for the WGS-84 coordinates h, Λ, and λ is now completed using the value of ξ.

From (A.31) the altitude above the ellipsoid above mean sea level is

$$h = \rho(\xi - 1) \tag{A.35}$$

To use this expression, ρ must be evaluated from the ECEF coordinates. From (A.29) and (A.31), obtain the sum of the squares of the components of the unit vector (u_X, u_Y, u_Z) in terms of (X, Y, Z). Multiplying this by ρ^2 and using (A.30) yields

$$\rho^2 = a^2 + \frac{e^2 Z^2}{\xi - e^2} \tag{A.36}$$

With this last result, h can be obtained from (A.35).

The longitude and latitude are obtained from the following two expressions, which are obtained from (A.26), (A.29) and (A.31).

$$\lambda = \sin^{-1}\left(\frac{Z}{\rho(\xi - e^2)}\right) \tag{A.37}$$

$$\Lambda = \tan^{-1}\left(\frac{Y}{X}\right) \tag{A.38}$$

3.6 Gravity Model

For the gravity model, $\bar{g}$ is by definition pointing perpendicular to the local ellipsoidal surface and thus only has a *Z* component in the geodetic reference frame. Gravity includes the combined effects of gravitation and the centrifugal acceleration from the Earth's rotation about its axis.

The gravity vector is $\bar{g} = (0,0,g)^{\mathrm{T}}$ in the geodetic reference frame. In ECEF coordinates, this gives at the surface of the Earth ellipsoid

$$\bar{g} = \begin{bmatrix} -\gamma \cos\lambda \cos\Lambda \\ -\gamma \cos\lambda \sin\Lambda \\ -\gamma \sin\lambda \end{bmatrix} \tag{A.39}$$

where γ is defined on the surface of the ellipsoid by

$$\gamma = \gamma_e \left(1 + g_1 \sin^2\lambda\right) \Big/ \sqrt{1 - e^2 \sin^2\lambda} \tag{A.40}$$

Gravity anomalies could be added to (A.40) but will be neglected here. γ_e is the acceleration of gravity at the equator of the WGS-84 ellipsoid and g_1 is the second order gravity coefficient which is given by

$$g_1 = \frac{b\gamma_p}{a\gamma_e} - 1 \tag{A.41}$$

where: *a* is the equatorial radius of the Earth reference ellipse,
b is the polar radius of the Earth reference ellipse,
γ_p is the acceleration of gravity at the poles of the WGS-84 ellipsoid.

For use in the 6/7 DOF, (A.39) needs to be corrected for the altitude *h* of the projectile

$$\bar{g}(h,\lambda) = \bar{g}\left(1-\frac{2}{a}\left(1+f+\frac{\Omega_E^2 a^2 b}{GM}-2f\sin^2\lambda\right)h+\frac{3}{a^2}h^2\right) \tag{A.42}$$

where Ω_E is the angular rate of the Earth's rotation.

3.7 Coriolis acceleration

The Coriolis acceleration in the ECEF earth-fixed rotating frame is

$$\bar{A}_C = -2\bar{\Omega}_E \times \bar{U} \tag{A.43}$$

where $\bar{\Omega}_E$ is the Earth's angular velocity and $\bar{U}$ is the velocity of the projectile with respect to ECEF frame.

The Earth's angular velocity vector is defined in the fire control system by

$$\bar{\Omega}_E = \begin{bmatrix} \omega_{E_X} \\ \omega_{E_Y} \\ \omega_{E_Z} \end{bmatrix} = \Omega_E \begin{bmatrix} \cos\lambda\cos AZ \\ \sin\lambda \\ -\cos\lambda\sin AZ \end{bmatrix} \tag{A.44}$$

where *AZ* is the azimuth with respect to north and λ is the geodetic latitude.

3.8 List of symbols

Symbol	Definition	Unit
a	Semi-major axis of reference ellipse, equatorial radius of Earth: 6378137.0000 meters.	*m*
$\bar{A}_C$	Coriolis acceleration vector.	m/s^2
AZ	Azimuth with respect to north.	*deg*
b	Semi-minor axis of reference ellipse, polar radius of Earth: 6356752.3142 meters.	*m*
d	Reference diameter of projectile.	*m*
e	Ellipsoidal eccentricity of the Earth: $e = \sqrt{1-(b/a)^2}$	-
f	Ellipsoidal flattening of the Earth: 1/298.257223563	-
$\bar{g}(h,\lambda)$	Acceleration of gravity (including centrifugal acceleration due to Earth's rotation) at latitude λ and altitude *h* in ECEF coordinates.	m/s^2
g_1	Second order gravity coefficient.	-
GM	Earth's gravitational constant: 3986004.418×10^8	m^3/s^2
h	Altitude of projectile. Shortest distance to reference ellipsoid.	*m*
$\bar{r}$	ECEF position vector of projectile. Components are *X*, *Y* and *Z*.	*m*
r_λ	Radius of Earth WGS-84 ellipsoid at latitude λ.	*m*
$\bar{U}$	Velocity vector of projectile with respect to ECEF frame.	*m/s*
X, *Y*, *Z*	ECEF coordinates of projectile.	*m*

γ_e	Acceleration of gravity at the equator of the WGS-84 ellipsoid: 9.7803267714 m/s^2	*m/s*^{2}
γ_p	Acceleration of gravity at the poles of the WGS-84 ellipsoid: 9.8321863685 m/s^2	*m/s*^{2}
Δt	Integration time step.	*s*
λ	Geodetic latitude (positive in northern hemisphere, negative in southern hemisphere).	*deg*
λ'	Geocentric latitude (positive in northern hemisphere, negative in southern hemisphere).	*deg*
Λ	Celestial longitude.	*deg*
$\omega_{E_X}, \omega_{E_Y}, \omega_{E_Z}$	ECEF components of Earth's angular velocity vector.	*rad/s*
$\overline{\Omega}_E$	Earth's angular velocity vector. Magnitude Ω_E: 7.292115 x 10^{-5} rad/s	*rad/s*

ANNEX B PROJECTILE AERODYNAMICS

1. Introduction

The following is a discussion of format for the use of aerodynamic coefficients for calculating the force and moment components in the 6 degrees of freedom (DOF) simulation. The body-fixed coordinate system is a right-handed orthonormal frame located at the center of mass *G*. Following the common convention in missile aerodynamics, *x* is positive forward looking from the rear toward the nose of the projectile, *y* is positive right and *z* is positive down. See Figure B.1. Roll is positive clockwise looking forward, a positive pitch moves the nose upward and a positive yaw moves the nose rightward. Roll is zero when the y-axis is pointing to the right in the horizontal plane.

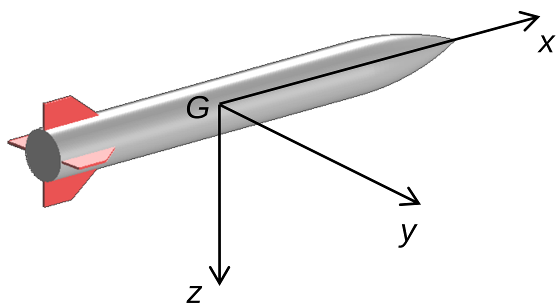

Figure B.1: Body-Fixed Coordinates System

Let $\overline{U}$ be the velocity vector of the projectile's center of mass with respect to Earth-fixed (ECEF) frame. Let $\overline{W}$ be the wind velocity vector at the center of mass with respect to ECEF frame. The air-relative velocity of the projectile is denoted by $\overline{V}$ and is defined as

$$\overline{V} = \overline{U} - \overline{W} \quad \text{(B.1)}$$

The x, y and z components of $\overline{V}$ in the body-fixed system are denoted by V_x, V_y and V_z and the magnitude of $\overline{V}$ is denoted by *V* (air speed).

Using the above notations, the angles of attack in the pitch and yaw planes are defined symmetrically as follows

$$\alpha = \tan^{-1}\left(\frac{V_z}{V_x}\right) \tag{B.2}$$

$$\alpha_y = \tan^{-1}\left(\frac{V_y}{V_x}\right) \tag{B.3}$$

The angle of sideslip is defined by

$$\beta = \sin^{-1}\left(\frac{V_y}{V}\right) \tag{B.4}$$

The total angle of attack between $\overline{V}$ and the *x*-axis is defined by

$$\alpha_{tot} = \cos^{-1}\left(\frac{V_x}{V}\right) \tag{B.5}$$

The total angle of attack plane is defined by $\overline{V}$ and the *x*-axis. The aerodynamic roll angle ϕ_A is the angle between the total angle of attack plane and the *xz*-plane. ϕ_A is zero when $\overline{V}$ is pointing downward in the *xz*-plane and it increases clockwise as follows

$$\phi_A = \tan^{-1}\left(\frac{-V_y}{V_z}\right) \tag{B.6}$$

The orientation of the velocity vector with respect to the body-fixed frame can thus be defined with any of the following pairs: (α, α_y), (α, β) or (α_{tot}, ϕ_A).

The aerodynamic forces and moments will be defined according to three cases: projectiles with rotational symmetry, isolated control surfaces and projectiles without rotational symmetry.

In the following sections, the aerodynamic coefficients are defined in compliance with STANAG 4355. The arguments of these coefficients are given as usually provided from wind tunnel data, typically just the Mach number and angle of attack. However, the simulation will be flexible enough for the user to increase the number of independent variables.

2. Projectiles with rotational symmetry

For projectiles with rotational symmetry, the aerodynamic forces and moments are defined according to the common convention in exterior ballistics, in compliance with STANAG 4355.

In this case, the aerodynamic coefficients are described by the general expression

$$C_* = C_*(\mathcal{M}, \mathcal{R}e, \alpha_{\text{tot}}) \tag{B.7}$$

where: $\mathcal{M}$ is the Mach number,
$\mathcal{R}e$ is the Reynolds number.

The derivative of the aerodynamic coefficient with respect to the total angle of attack is denoted by C_{*_α} and is defined by

$$C_* = C_{*_\alpha} \sin\alpha_{\text{tot}} \tag{B.8}$$

NOTE: The aerodynamic coefficient notations used in this section comply with the symbols defined in Table III-1 of STANAG 4355.

Aerodynamic coefficients can be changed using multiplicative and additive factors. This may be useful to fit an observed trajectory or to change the aerodynamic properties of the projectile during flight. In the following sections (2.1 to 2.9), the actual value of the aerodynamic coefficient is denoted by $\hat{C}_*$ and is defined by

$$\hat{C}_* = f_{C*} C_* + f_{\Delta C*} \Delta C_* \tag{B.9}$$

where: C_* is the baseline value,
ΔC_* is the (optional) increment value,
f_{C*} and $f_{\Delta C*}$ are scale factors.

2.1 The drag force is given by

$$\overline{DF} = -\frac{1}{2}\rho S \hat{C}_D V \overline{V} \tag{B.10}$$

where: ρ is the air density,

$\overline{V}$ is the projectile velocity vector with respect to the air (*V* is the magnitude of the vector),

S is the projectile reference area (the default usage is $S = \pi d^2/4$ where *d* is the body diameter),

$\hat{C}_D$ is the drag force coefficient.

2.2 <u>The lift force is given by</u>

$$\overline{LF} = \frac{1}{2}\rho S \hat{C}_{L_\alpha} \left(\overline{V} \times \left(\overline{x} \times \overline{V}\right)\right) \qquad \text{(B.11)}$$

where: $\overline{x}$ is the unit vector of the projectile axis of symmetry,

$\hat{C}_{L_\alpha}$ is the derivative of the lift force coefficient.

2.3 <u>The overturning moment is given by</u>

$$\overline{OM} = \frac{1}{2}\rho S d \hat{C}_{M_\alpha} V \left(\overline{V} \times \overline{x}\right) \qquad \text{(B.12)}$$

where: *d* is the projectile diameter,

$\hat{C}_{M_\alpha}$ is the derivative of the overturning moment coefficient.

2.4 <u>The pitch damping force is given by</u>

$$\overline{PDF} = \frac{1}{2}\rho S d (\hat{C}_{N_q} + \hat{C}_{N_{\dot{\alpha}}}) V \left(\overline{\omega} \times \overline{x}\right) \qquad \text{(B.13)}$$

where: $\overline{\omega}$ is the angular velocity of the projectile,

$\hat{C}_{Nq}$ is the pitch damping force coefficient due to pitch and yaw motion,

$\hat{C}_{N_{\dot{\alpha}}}$ is the pitch damping force coefficient due to $\dot{\alpha}$.

2.5 <u>The pitch damping moment is given by</u>

$$\overline{PDM} = \frac{1}{2}\rho S d^2 (\hat{C}_{M_q} + \hat{C}_{M_{\dot{\alpha}}}) V \left(\overline{x} \times \left(\overline{\omega} \times \overline{x}\right)\right) \qquad \text{(B.14)}$$

where: $\hat{C}_{M_q}$ is the pitch damping moment coefficient due to pitch and yaw motion,

$\hat{C}_{M_{\dot{\alpha}}}$ is the pitch damping moment coefficient due to $\dot{\alpha}$.

Note: Equations (B.13) and (B.14) are commonly used approximations of the pitch damping force and moment, assuming that the pitching velocity q and the rate of change of total angle of attack $\dot{\alpha}$ are virtually identical in practice.

2.6 The Magnus force is given by

$$\overline{MF} = \frac{1}{2}\rho S\left(\frac{pd}{V}\right)\hat{C}_{mag-f}\, V\left(\overline{V}\times\overline{x}\right) \qquad \text{(B.15)}$$

where: p is the spin of the projectile,
$\hat{C}_{mag-f}$ is the Magnus force coefficient.

2.7 The Magnus moment is given by

$$\overline{MM} = \frac{1}{2}\rho S d\left(\frac{pd}{V}\right)\hat{C}_{mag-m}\, V\left(\overline{x}\times\left(\overline{V}\times\overline{x}\right)\right) \qquad \text{(B.16)}$$

where: $\hat{C}_{mag-m}$ is the Magnus moment coefficient.

2.8 The rolling moment is given by

$$\overline{RM} = \frac{1}{2}\rho S\, d\, \delta_F\, \hat{C}_{l_\delta}\, V^2\,\overline{x} \qquad \text{(B.17)}$$

where: δ_F is the fin cant angle,
$\hat{C}_{l_\delta}$ is the fin cant moment coefficient.

2.9 The spin damping moment is given by

$$SDM = \frac{1}{2}\rho S\, d\left(\frac{p\,d}{V}\right)\hat{C}_{spin}\, V^2\,\overline{x} \qquad \text{(B.18)}$$

where: $\hat{C}_{spin}$ is the spin damping moment coefficient.

3. Isolated control surfaces

Individual movable surfaces can be attached to rotationally symmetric projectiles. These small surfaces generate additional lift and drag forces and related moments.
The position and the orientation of the control surface no. i is defined in the body-fixed frame by the position of the center of pressure and the individual cant angle δ_{F_i} as illustrated by Figure B.2.

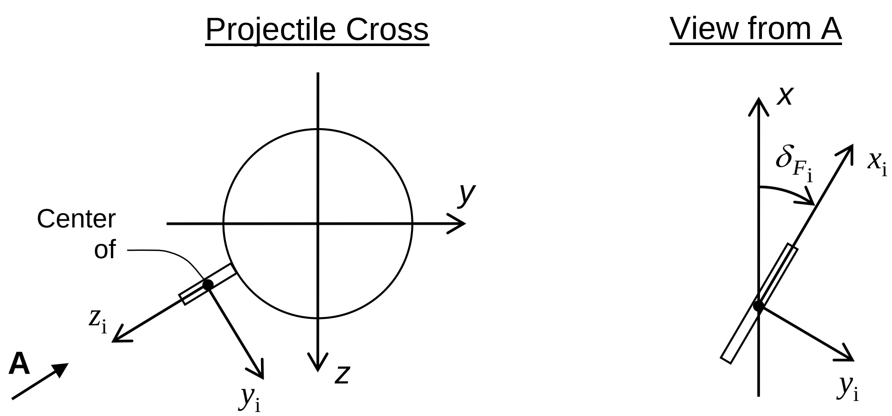

Figure B.2: Position and Orientation of Control Surface no. i

The aerodynamic force generated by the surface is given by

$$\overline{F}_i = \frac{1}{2}\rho S_i \left(-C_{D_i} V_i \overline{V}_i + C_{L_{\alpha i}} \left(\overline{V}_i \times \left(\overline{x}_i \times \overline{V}_i \right) \right) \right) \quad \text{(B.19)}$$

where: S_i is the area of the control surface,

$\overline{V}_i$ is the component of the air relative velocity of the center of pressure which is tangent to the body surface,

C_{D_i} is the drag coefficient of the control surface,

$C_{L_{\alpha i}}$ is the lift coefficient derivative of the control surface.

The related moment is simply given by

$$\overline{M}_i = \overline{r}_i \times \overline{F}_i \quad \text{(B.20)}$$

where: $\bar{r}_i$ is the vector defined from the projectile center of mass to the surface center of

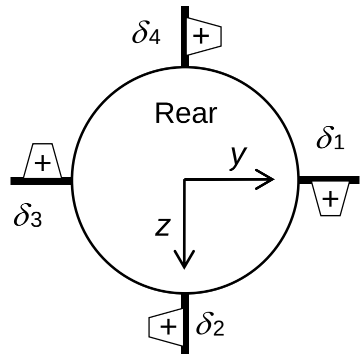

pressure.

4. Projectiles without rotational symmetry

For projectiles without rotational symmetry, the aerodynamic forces and moments are defined according to the common convention in missile aerodynamics.

In this case, the effect of the aerodynamic control surfaces of the projectile (e.g. tail fins or canards) is described using global control surfaces. The general expression of the aerodynamic coefficients is given by

$$C_* = C_*(\mathcal{M}, \mathcal{R}e, \alpha, \alpha_y, \delta_{elevator}, \delta_{rudder}, \delta_{aileron}) \quad \text{(B.21)}$$

where: $\delta_{elevator}$ is the control surface deflection that produces a pitching moment,
δ_{rudder} is the control surface deflection that produces a yawing moment,
$\delta_{aileron}$ is the control surface deflection that produces a rolling moment.

The exact format for dependence on independent variables, the positions of the control surfaces and the definitions of the control surface deflections $\delta_{elevator}$, δ_{rudder} and $\delta_{aileron}$ might vary for different projectile concepts. Two methods can be used to define the global deflection parameters according to the deflections of the isolated control surfaces (fins or canards).

Figure B.3: Positive Deflection of Control Surfaces (Method 1)

Method 1. Consider the positive deflection of the isolated control surfaces defined by Figure B.3. In this case, the global control deflections are computed as follows:

$$\delta_{\mathrm{elevator}} = \tfrac{1}{2}(\delta_1 - \delta_3)\,,\ \delta_{\mathrm{rudder}} = \tfrac{1}{2}(\delta_2 - \delta_4)\,,\ \delta_{\mathrm{aileron}} = -\tfrac{1}{4}(\delta_1 + \delta_2 + \delta_3 + \delta_4) \qquad \text{(B.22)}$$

Method 2. Consider the positive deflection of the isolated control surfaces defined by Figure B.4. In this case, the global control deflections are computed as follows:

$$\delta_{elevator} = \tfrac{1}{4}(\delta_1 + \delta_2 + \delta_3 + \delta_4)\,, \delta_{rudder} = \tfrac{1}{4}(-\delta_1 + \delta_2 - \delta_3 + \delta_4)\,, \delta_{aileron} = \tfrac{1}{4}(-\delta_1 - \delta_2 + \delta_3 + \delta_4) \qquad \text{(B.23)}$$

Figure B.4: Positive Deflection of Control Surfaces (Method 2)

Let *X*, *Y* and *Z* denote the x, y and z body-fixed frame components of the total aerodynamic force applied on the projectile. These components, including form factors (scale factors), are

$$X = \frac{1}{2}\rho V^2 S\, f_{CX}\, C_X\left(\mathcal{M}, \mathcal{R}e, \alpha, \alpha_{\mathrm{y}}, \delta_{\mathrm{elevator}}, \delta_{\mathrm{rudder}}\right) \qquad \text{(B.24)}$$

$$Y = \frac{1}{2}\rho V^2 S\, f_{CY}\, C_Y\left(\mathcal{M}, \mathcal{R}e, \alpha_{\mathrm{y}}, \delta_{\mathrm{rudder}}\right) \qquad \text{(B.25)}$$

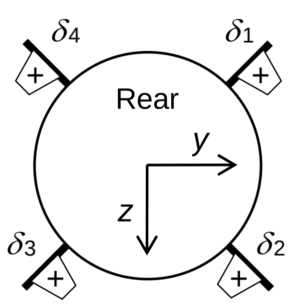

$$Z = \frac{1}{2}\rho V^2 S\, f_{CZ}\, C_Z\left(\mathcal{M}, \mathcal{R}e, \alpha, \delta_{\mathrm{elevator}}\right) \qquad \text{(B.26)}$$

Let *L*, *M* and *N* denote the x, y, and z body-fixed frame components of the total aerodynamic moment applied on the projectile. These components, including form factors (scale factors), are

$$L = \frac{1}{2}\rho V^2 S\, d\left[f_{Cl}\, C_l\left(\mathcal{M},\mathcal{R}e,\delta_{\text{aileron}}\right) + \left(\frac{p\,d}{V}\right) f_{Cspin}\, C_{spin}\left(\mathcal{M},\mathcal{R}e\right)\right] \tag{B.27}$$

$$M = \frac{1}{2}\rho V^2 S\, d\left[f_{Cm}\, C_m\left(\mathcal{M},\mathcal{R}e,\alpha,\delta_{\text{elevator}}\right) + \left(\frac{q\,d}{V}\right) f_{CM_q}\, C_{M_q}\left(\mathcal{M},\mathcal{R}e\right)\right] \tag{B.28}$$

$$N = \frac{1}{2}\rho V^2 S\, d\left[f_{Cn}\, C_n\left(\mathcal{M},\mathcal{R}e,\alpha_{\text{y}},\delta_{\text{rudder}}\right) + \left(\frac{r\,d}{V}\right) f_{CM_r}\, C_{M_r}\left(\mathcal{M},\mathcal{R}e\right)\right] \tag{B.29}$$

The dependence on the equivalent aerodynamic control surface deflections can be separated from the rest of the projectile (which often has rotational symmetry) using specific increment coefficients denoted by C_{*_*} in the following expressions

$$\begin{aligned} X = \frac{1}{2}\rho V^2 S\big[\, & f_{CX}\, C_X\left(\mathcal{M},\mathcal{R}e\right) + f_{CX\_E}\, C_{X\_E}\left(\mathcal{M},\mathcal{R}e,\alpha,\delta_{\text{elevator}}\right) \\ & + f_{CX\_R}\, C_{X\_R}\left(\mathcal{M},\mathcal{R}e,\alpha_{\text{y}},\delta_{\text{rudder}}\right)\big] \end{aligned} \tag{B.30}$$

$$\begin{aligned} Y = \frac{1}{2}\rho V^2 S\big[\, & f_{CY}\, C_Y\left(\mathcal{M},\mathcal{R}e\right) + f_{CY\_E}\, C_{Y\_E}\left(\mathcal{M},\mathcal{R}e,\alpha,\delta_{\text{elevator}}\right) \\ & + f_{CY\_R}\, C_{Y\_R}\left(\mathcal{M},\mathcal{R}e,\alpha_{\text{y}},\delta_{\text{rudder}}\right)\big] \end{aligned} \tag{B.31}$$

$$\begin{aligned} Z = \frac{1}{2}\rho V^2 S\big[\, & f_{CZ}\, C_Z\left(\mathcal{M},\mathcal{R}e\right) + f_{CZ\_E}\, C_{Z\_E}\left(\mathcal{M},\mathcal{R}e,\alpha,\delta_{\text{elevator}}\right) \\ & + f_{CZ\_R}\, C_{Z\_R}\left(\mathcal{M},\mathcal{R}e,\alpha_{\text{y}},\delta_{\text{rudder}}\right)\big] \end{aligned} \tag{B.32}$$

$$\begin{aligned} L = \frac{1}{2}\rho V^2 S\, d\big[\, & f_{Cl}\, C_l\left(\mathcal{M},\mathcal{R}e\right) + f_{Cl\_A}\, C_{l\_A}\left(\mathcal{M},\mathcal{R}e,\delta_{\text{aileron}}\right) \\ & + \left(\frac{p\,d}{V}\right) f_{Cspin}\, C_{spin}\left(\mathcal{M},\mathcal{R}e\right)\big] \end{aligned} \tag{B.33}$$

$$M = \frac{1}{2}\rho V^2 S\, d\Big[\, f_{Cm}\, C_m(\mathcal{M},\mathcal{R}e) + f_{Cm\_E}\, C_{m\_E}(\mathcal{M},\mathcal{R}e,\alpha,\delta_{\text{elevator}}) + f_{Cm\_R}\, C_{m\_R}(\mathcal{M},\mathcal{R}e,\alpha_{\text{y}},\delta_{\text{rudder}}) + \left(\frac{q\,d}{V}\right) f_{CM_q}\, C_{M_q}(\mathcal{M},\mathcal{R}e)\Big] \quad \text{(B.34)}$$

$$N = \frac{1}{2}\rho V^2 S\, d\Big[\, f_{Cn}\, C_n(\mathcal{M},\mathcal{R}e) + f_{Cn\_E}\, C_{n\_E}(\mathcal{M},\mathcal{R}e,\alpha,\delta_{\text{elevator}}) + f_{Cn\_R}\, C_{n\_R}(\mathcal{M},\mathcal{R}e,\alpha_{\text{y}},\delta_{\text{rudder}}) + \left(\frac{r\,d}{V}\right) f_{CM_r}\, C_{M_r}(\mathcal{M},\mathcal{R}e)\Big] \quad \text{(B.35)}$$

5. Aerodynamic coefficients table look-up

Aerodynamic coefficients are provided as tables with multiple independent variables such as Mach number, Reynolds number, total angle of attack and aerodynamic roll angle (or pitch and yaw angles of attack), control surface deflection angles. The dependency on Reynolds number may be expressed using a separate scale function depending on the altitude.

These tables are used as multi-linear interpolated look up. Alternatively, the table lookups can be done using polynomials in powers of the angle of attack. This is the approach currently used in the modified point-mass model. See Table III-1 in STANAG 4355. For example:

$$C_D(\mathcal{M},\alpha_{\text{tot}}) = C_{D_0}(\mathcal{M}) + C_{D_{\alpha^2}}(\mathcal{M})\sin^2\alpha_{\text{tot}} + C_{D_{\alpha^4}}(\mathcal{M})\sin^4\alpha_{\text{tot}} \quad \text{(B.36)}$$

6. Comparison of aerodynamic symbols

This STANAG document explicitly uses the quantity (*pd*/*v*). The following equivalences are provided to avoid confusion with the NACA aeroballistic system that uses the quantity (*pd*/2*v*).

$C_{mag\text{-}f} = C_{N_{p\alpha}}$ for data nondimensionalized using *pd/v* (B.37)

$= (1/2)\, C_{y_{p\alpha}}$ for data nondimensionalized using *pd/*2*v* (B.38)

$C_{mag\text{-}m} = C_{M_{p\alpha}}$ for data nondimensionalized using *pd/v* (B.39)

	$= (1/2)\ C_{n_{p\alpha}}$	for data nondimensionalized using *pd/2v*	(B.40)
C_{spin}	$= C_{l_p}$	for data nondimensionalized using *pd/v*	(B.41)
	$= (1/2)\ C_{l_p}$	for data nondimensionalized using *pd/2v*	(B.42)
C_{Mq}		for data nondimensionalized using *pd/v*	(B.43)
	$= (1/2)\ C_{mq}$	for data nondimensionalized using *pd/2v*	(B.44)

The aerodynamic force in the angle of attack plane can be decomposed into the sum of the lift and drag forces or into the sum of the normal and axial forces. See Figure B.5.

Figure B.5: Lift, Drag, Normal and Axial Forces

The drag force is defined by (B.9) and the lift force is defined by (B.10).

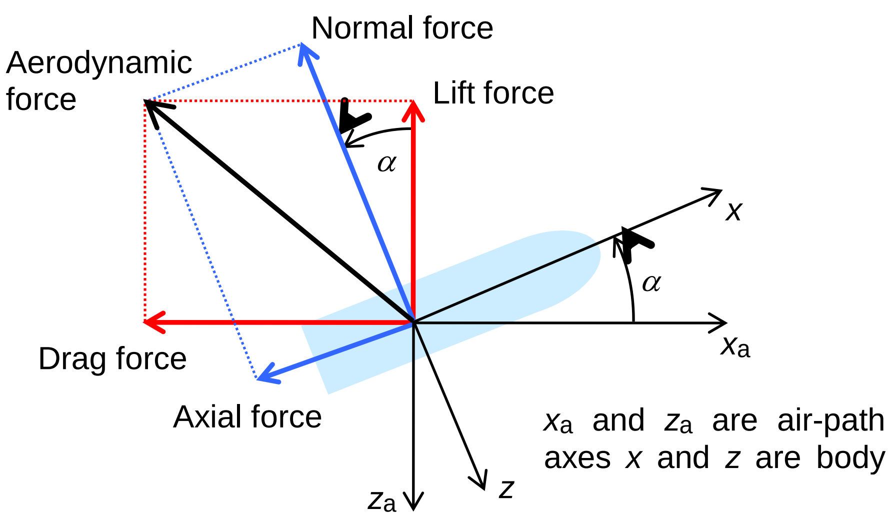

The axial force is given by

$$\overline{AF} = \frac{1}{2}\rho S \hat{C}_X V^2 \overline{x} \tag{B.45}$$

The normal force is given by

$$\overline{NF} = \frac{1}{2}\rho\, S\, \hat{C}_{N_\alpha}\, V\left(\bar{x}\times\left(\bar{x}\times\bar{V}\right)\right) \tag{B.46}$$

The equivalence between the lift (C_L), drag (C_D), normal (C_N) and axial (C_X) coefficients is therefore defined by

$$\begin{bmatrix} C_N \\ -C_X \end{bmatrix} = \begin{bmatrix} \cos\alpha & \sin\alpha \\ -\sin\alpha & \cos\alpha \end{bmatrix}\begin{bmatrix} C_L \\ C_D \end{bmatrix} \tag{B.47}$$

7. List of symbols for aerodynamics

Symbol	Definition	Unit
C_*	Generic aerodynamic coefficient (baseline value).	-
$\hat{C}_*$	Generic aerodynamic coefficient (actual value).	-
$C_{*\alpha}$	Derivative of generic aerodynamic coefficient with respect to total angle of attack.	-
C_l	Rolling moment coefficient.	-
C_{l_A}	Rolling moment increment coefficient due to aileron deflection.	-
C_{l_δ}	Fin cant moment coefficient.	-
C_{l_p}	Spin damping moment coefficient normalized using $pd/2v$.	-
C_m	Pitching moment coefficient.	-
C_{M_α}	Derivative of the overturning moment coefficient.	-
C_{m_E}	Pitching moment increment coefficient due to elevator deflection.	-
C_{m_R}	Pitching moment increment coefficient due to rudder deflection.	-
$C_{mag\text{-}f}$	Magnus force coefficient normalized using pd/v.	-
$C_{mag\text{-}m}$	Magnus moment coefficient normalized using pd/v.	-
C_{m_q}	Pitch damping coefficient normalized using $qd/2v$.	-
C_{M_q}	Pitch damping coefficient normalized using qd/v.	-
C_{m_r}	Yaw damping coefficient normalized using $rd/2v$.	-
C_{M_r}	Yaw damping coefficient normalized using rd/v.	-

C_n	Yawing moment coefficient.	-
C_{n_E}	Yawing moment increment coefficient due to elevator deflection.	-
C_{n_R}	Yawing moment increment coefficient due to rudder deflection.	-
C_{n_p}	Magnus moment coefficient normalized using $pd/2v$.	-
C_N	Normal force coefficient.	-
C_{spin}	Spin damping moment coefficient normalized using pd/v.	-
C_X	Axial force coefficient.	-
C_{X_E}	Axial force increment coefficient due to elevator deflection.	-
C_{X_R}	Axial force increment coefficient due to rudder deflection.	-
C_Y	Lateral force coefficient.	-
C_{Y_E}	Lateral force increment coefficient due to elevator deflection.	-
C_{Y_R}	Lateral force increment coefficient due to rudder deflection.	-
C_Z	Vertical force coefficient.	-
C_{Z_E}	Vertical force increment coefficient due to elevator deflection.	-
C_{Z_R}	Vertical force increment coefficient due to rudder deflection.	-
C_{Y_p}	Magnus force coefficient normalized using $pd/2v$.	-
d	Reference length (typically, caliber of the projectile).	m
f_{C*}	Scale factor for aerodynamic coefficient denoted by C_*.	-

$f_{\Delta C*}$	Scale factor for aerodynamic coefficient increment denoted by ΔC_*.	-
$\mathcal{M}$	Free stream Mach number.	-
p, q, r	x, y, z components of the angular velocity vector of the projectile in body-fixed frame.	*rad/s*
$\mathcal{Re}$	Free stream Reynolds number.	-
S	Reference area (typically, cross section of the projectile).	m^2
$\overline{U}$	Projectile velocity vector with respect to ECEF frame.	*m/s*
$\overline{V}$	Projectile velocity vector with respect to air.	*m/s*
V_x, V_y, V_z	x, y, z components of $\overline{V}$ in body-fixed frame.	*m/s*
$\overline{W}$	Wind velocity vector with respect to ECEF frame.	*m/s*
X_{CG}	x position of the projectile's center of mass in body-fixed frame.	*m*
X_{CP_M}	x position of the projectile's center of pressure for Magnus force in body-fixed frame.	*m*
X_{CP_N}	x position of the projectile's center of pressure for normal force in body-fixed frame.	*m*
α	Angle of attack.	*rad*
α_{tot}	Total angle of attack.	*rad*
α_y	Yaw-like angle of attack.	*rad*
β	Angle of sideslip.	*rad*
ΔC_*	Generic aerodynamic coefficient increment.	-
$\delta_{aileron}$	Aileron deflection.	*rad*

$\delta_{elevator}$	Elevator deflection.	*rad*
δ_F	Fin cant angle.	*rad*
δ_{rudder}	Rudder deflection.	*rad*
ρ	Air density.	kg/m^3
ϕ_A	Aerodynamic roll angle.	*rad*

ANNEX C COORDINATE CONVERSION REQUIRED BY COURSE CORRECTING FUZES

1. Introduction

This document describes the equations for the coordinate conversions required by course correcting fuzes. There are two coordinate conversions that are required to support course correcting fuzes: gun frame to North, East, Down (NED) and Lat/Long to Earth-Center, Earth-Fixed (ECEF).

The gun frame to NED conversion starts with vectors oriented in a coordinate frame with an origin at mean sea level directly below the trunnion the weapon being fired, where the x_1 axis is tangent to the earth's surface at the origin and points along the gun-target line, the x_2 axis is in the vertical plane perpendicular to the surface of the earth (or ellipsoidal representation of the surface), and the x_3 axis is perpendicular to the plane formed by the other two axes so as to define a right hand Cartesian coordinate system. The x_1 axis is positive in the direction of target, the x_2 axis is positive above the surface of the earth, and the x_3 axis is positive to the right of the gun location when facing the target. The gun-target azimuth is the clockwise angular measure between true north and the gun-target line taken at the gun. The transformation converts to a reference frame where the vectors are represented with the origin of the coordinate frame located at the target, and the axes of the system pointing northward, eastward, and downward. The North-East plane is tangent to the WGS84 ellipsoid at the target. Thus the downward axis is perpendicular to the WGS84 ellipsoid at the target. The North axis is positive north of the target, the East axis is positive east of the target, and the Down axis is positive for points below the target.

The Lat/Long to ECEF conversion, used in the gun frame to NED transformation, converts coordinates given in terms of latitude, longitude, and altitude with respect to the WGS84 ellipsoid to a coordinate system where the origin is the mass center of the earth and the axes are: out through the intersection of the equator and the prime meridian, the rotational axis of the earth, and the final axis is perpendicular to the plane formed by the other two axes so as to satisfy the right-hand rule. The earth is modeled as an ellipsoid as described in the earth model WGS84.

2. Gun Frame To NED Conversion

A. Inputs

The following data are required as input:

1. Gun-target azimuth, Az_{gt} (radians) clockwise with respect to true north
2. Projectile position with respect to gun frame (wrt/ MSL), $\bar{x}$ (m)
3. Projectile velocity components with respect to gun frame, $\bar{u}$ (m/s)
4. Latitude of target, ϕ_{target} (radians)
5. Latitude of gun, ϕ_{gun} (radians)
6. Longitude of target, λ_{target} (radians)
7. Longitude of gun, λ_{gun} (radians)
8. Height of target above WGS84 ellipsoid, h_{target} (m)
9. Height of gun above WGS84 ellipsoid, h_{gun} (m)
10. Height of gun above mean sea level, alt_{gun} (m)

B. Known Values

From the WGS84 model:

$$R_{equator} = 6{,}378{,}137 \text{ meters}$$
$$f = \frac{1}{298.257223563}$$
$$e^2 = 1 - (1 - f)^2 \cong 0.006694379990141$$

C. Determine ECEF Coordinates

Compute the ECEF coordinates such that the z-axis points northward along the Earth's rotation axis, the x-axis points outward along the intersection of the Earth's equatorial plane and prime meridian, and the y-axis points into the eastward quadrant, perpendicular to the x-z plane so as to satisfy the right-hand rule.

$$N_L = \frac{R_{equator}}{\sqrt{1 - e^2 \sin^2(\phi_L)}} \tag{C.1}$$

$$\bar{r}_L = \begin{bmatrix} X \\ Y \\ Z \end{bmatrix}_L = \begin{bmatrix} (N_L + h_L)\cos(\phi_L)\cos(\lambda_L) \\ (N_L + h_L)\cos(\phi_L)\sin(\lambda_L) \\ (N_L(1 - e^2) + h_L)\sin(\phi_L) \end{bmatrix} \tag{C.2}$$

Where the subscript L can be either the gun or target location.

D. Computation of Direction Cosine Matrix

The direction cosine matrix (DCM) used to transform ECEF coordinates to the NED frame is:

$$\left[\mathrm{DCM_L}\right] = \begin{bmatrix} -\sin(\phi_\mathrm{L})\cos(\lambda_\mathrm{L}) & -\sin(\phi_\mathrm{L})\sin(\lambda_\mathrm{L}) & \cos(\phi_\mathrm{L}) \\ -\sin(\lambda_\mathrm{L}) & \cos(\lambda_\mathrm{L}) & 0 \\ -\cos(\phi_\mathrm{L})\cos(\lambda_\mathrm{L}) & -\cos(\phi_\mathrm{L})\sin(\lambda_\mathrm{L}) & -\sin(\phi_\mathrm{L}) \end{bmatrix} \quad \text{(C.3)}$$

Again the subscript L is either the gun or target location.

E. Determine the Projectile Location in a Gun-Centered NED Frame

This is accomplished by rotating about the opposite of the gun-target azimuth about the x_2/Down axis.

$$\overline{\mathrm{x}}_{\mathrm{NED_{gun}}} = \begin{bmatrix} \mathrm{North_{gun}} \\ \mathrm{East_{gun}} \\ \mathrm{Down_{gun}} \end{bmatrix} = \begin{bmatrix} \cos(Az_\mathrm{gt}) & 0 & -\sin(Az_\mathrm{gt}) \\ \sin(Az_\mathrm{gt}) & 0 & \cos(Az_\mathrm{gt}) \\ 0 & -1 & 0 \end{bmatrix} \begin{bmatrix} x_1 \\ x_2 - alt_\mathrm{gun} \\ x_3 \end{bmatrix} \quad \text{(C.4)}$$

F. Determine the ECEF Vector Components from Gun-to-Projectile

Transform the projectile NED vector into a vector oriented in the ECEF frame using the gun's DCM.

$$\left[\mathrm{DCM_{gun}}\right]\overline{\mathrm{X}}_\mathrm{gun} = \overline{\mathrm{x}}_{\mathrm{NED_{gun}}} \quad \text{(C.5)}$$

Note: Solve for $\overline{\mathrm{X}}_\mathrm{gun}$

G. Calculate the ECEF Vector Components from Target-to-Projectile

This is done by, first, finding the vector from the center of the ellipsoid to the projectile. This vector is simply the sum of the gun ECEF vector and the gun-to-projectile ECEF vector. Then by subtracting from this center-of-ellipsoid-to-projectile vector the target ECEF vector.

$$\overline{X}_{target} = \overline{r}_{gun} + \overline{X}_{gun} - \overline{r}_{target} \quad (C.6)$$

H. Obtain the Position of the Projectile in the NED Target-Centered Frame

Transform the target-to-projectile ECEF vector into a vector oriented in the target's NED frame using the target's DCM.

$$\overline{x}_{NED} = \left[DCM_{target}\right]\overline{X}_{target} \quad (C.7)$$

I. Obtain the Velocity of the Projectile in the NED Target-Centered Frame

This transformation is similar to the steps above.

1) Determine the Projectile Velocity in a Gun-Centered NED Frame

This is accomplished by rotating about the opposite of the azimuth to target about the x_2/Down axis.

$$\overline{u}_{NED_{gun}} = \begin{bmatrix} \dot{North}_{gun} \\ \dot{East}_{gun} \\ \dot{Down}_{gun} \end{bmatrix} = \begin{bmatrix} \cos(Az_{gt}) & 0 & -\sin(Az_{gt}) \\ \sin(Az_{gt}) & 0 & \cos(Az_{gt}) \\ 0 & -1 & 0 \end{bmatrix} \begin{bmatrix} u_1 \\ u_2 \\ u_3 \end{bmatrix} \quad (C.8)$$

2) Determine the ECEF Vector Components of the Projectile Velocity

Transform the projectile NED vector into a vector oriented in the ECEF frame using the gun's DCM.

$$\left[DCM_{gun}\right]\overline{U} = \overline{u}_{NED_{gun}} \quad (C.9)$$

Note: Solve for $\overline{U}$

3) Obtain the Velocity of the Projectile in the NED Target-Centered Frame

Transform the projectile ECEF vector into a vector oriented in the target's NED frame using the target's DCM.

$$\bar{u}_{NED} = \left[DCM_{target}\right]\overline{U} \qquad (C.10)$$

3. Computation Of Euler Angles In The Ned Frame

The Euler angles (ψ, θ) of the projectile velocity in the NED frame are:

$$\psi = \tan^{-1}\frac{u_E}{u_N} \qquad -\pi \le \psi \le \pi \qquad (C.11)$$

$$\theta = \tan^{-1}\frac{-u_D}{\sqrt{u_E^2 + u_N^2}} \qquad -\frac{\pi}{2} \le \theta \le \frac{\pi}{2} \qquad (C.12)$$

Where u_E, u_N and u_D are, respectively, the eastward, northward and downward components of projectile velocity in the target-centered NED frame.

4. List of Symbols

Symbol	Definition	Unit
alt_{gun}	altitude of the gun wrt/ mean sea level	*m*
Az_{gt}	gun-target azimuth	*rad*
DCM	direction cosine matrix	-
DCM_{gun}	direction cosine matrix to convert ECEF to NED for the gun	-
DCM_{target}	direction cosine matrix to convert ECEF to NED for the target	-
e	eccentricity	-
ECEF	earth-centered, earth-fixed coordinate system	-
f	flattening of the earth	-
h	height above WGS84 ellipsoid	*m*
h_{gun}	height of gun above WGS84 ellipsoid	*m*
h_{target}	height of target above WGS84 ellipsoid	*m*
MSL	mean sea level	-
N	distance from surface of ellipsoid to polar axis along line normal to the ellipsoid surface	*m*
$R_{equator}$	equatorial radius of the earth	*m*
$\bar{r}_{gun}$	ECEF position vector of gun	*m*
$\bar{r}_{target}$	ECEF position vector of target	*m*
$\bar{u}$	projectile velocity vector in the gun frame	*m/s*

u_1, u_2, u_3	components of projectile velocity in the gun frame	*m/s*
$\bar{u}_{NED}$	projectile velocity vector in target-centered NED frame	*m/s*
u_N, u_E, u_D	northward, eastward and downward components of projectile velocity in target-centered NED frame	*m/s*
$\bar{u}_{NED_{gun}}$	projectile velocity vector in gun-centered NED frame	*m/s*
$\bar{U}$	projectile velocity vector in earth-centered, earth-fixed coordinate system	*m/s*
x_1 axis	axis which runs from the gun to the target	-
x_2 axis	axis oriented perpendicular to the WGS84 model's surface of the earth	-
x_3 axis	axis oriented perpendicular to the x_1-x_2 plane so as to satisfy the right-hand rule	-
$\bar{x}$	projectile position vector in the gun frame	*m*
x_1, x_2, x_3	components of projectile position in the gun frame (x_2 component given wrt/ mean sea level)	*m*
$\bar{x}_{NED}$	projectile position vector in target-centered NED frame	*m*
$\bar{x}_{NED_{gun}}$	projectile position vector in gun-centered NED frame	*m*
$\bar{X}_{gun}$	gun-to-projectile vector in earth-centered, earth-fixed coordinate system	*m*
$\bar{X}_{target}$	target-to-projectile vector in earth-centered, earth-fixed coordinate system	*m*
$\bar{X}_{NED_{target}}$	projectile position vector in target-centered NED frame	*m*
λ	longitude	*rad*
λ_{gun}	longitude of gun	*rad*

$\lambda_{\mathrm{target}}$	longitude of target	*rad*
ϕ	geodetic latitude	*rad*
ϕ_{gun}	geodetic latitude of gun	*rad*
ϕ_{target}	geodetic latitude of target	*rad*

ANNEX D ADDITIONAL TERMS FOR ROCKET-ASSISTED AND BASE-BURN PROJECTILES METHOD 1

1. Introduction

This annex provides the equations required to simulate the flight of rocket-assisted projectiles and the specific equations required to simulate the flight of base-burn projectiles. This method is fully defined in ANNEX C to STANAG 4355. The differences are due to the use of body-fixed axes in the 6/7 DOF simulation rather than wind axes. That is, the body-fixed axes coordinates are X forward along body rotational symmetry axis, Y rightward, and the third axis Z completes a right hand set.

2. Equations I

2.1. Additional Terms for Spin-Stabilized Rocket-Assisted Projectiles

Add the thrust term T^* to the equation of motion of the center of mass of the projectile. T^* is added to F_X in the projectile's body-fixed or zero-p frame. The components F_Y and F_Z in the body-fixed frame are unaffected. The rest of this section is unchanged.

a. Thrust during the burning phase ($t_{DI} \leq t \leq t_B$) is as follows:

$$T^* = f_T T_R + (P_r - P)A_e, \qquad \text{(D.1)}$$

where:

$$T_R = T_{ST}\left(t_{DI_{ST}} - t_{B_{ST}}\right)/\left(t_{DI} - t_B\right), \qquad \text{(D.2)}$$

and

$$t^* = \left(t - t_{DI}\right)\left[\left(t_{DI_{ST}} - t_{B_{ST}}\right)/\left(t_{DI} - t_B\right)\right] + t_{DI_{ST}} \qquad \text{(D.3)}$$

b. Zero yaw drag coefficient during the burning phase ($t_{DI} \leq t \leq t_B$) is $C_{D_{o_T}}$.

c. Mass of the projectile is given by:

mass at $t = 0$ is $m = m_0$ (D.4)

for $t < t_{DI}$

$$\dot{m} = -m_{DI} / t_{DI} \qquad \text{(D.5)}$$

mass at $t = t_{DI}$ is $m = m_0 - m_{DI} - m_{DOB}$ (D.6) for $t_{DI} \le t < t_B$

$$\dot{m} = -T_R / I_{SP} \tag{D.7}$$

for $t \ge t_B$

$$\dot{m} = 0 \tag{D.8}$$

$$m = m_B \tag{D.9}$$

where:

$$m_B = m_0 - m_{DI} - m_{DOB} - m_f \tag{D.10}$$

2.2. Additional Terms for Spin-Stabilized Base-Burn Projectiles

a. The change in acceleration due to the base drag reduction of a base-burn motor, *BB*, during burning ($t_{DI} \le t$ and $m \ge m_B$) is added to F_X/m in the equation (8) or (12) for the center of mass of the projectile:

$$BB = +\left[\frac{\left(\frac{\pi}{8}\right)\rho\, d^2\, v^2\, C_{X_{BB}}\; f(I)\, f(i_{BB}, MT)}{m}\right] \tag{D.11}$$

F_Y and F_Z in the 6/7 DOF body-fixed frame are unchanged.

b. The coefficient $C_{x_{BB}}$ is the drag reduction coefficient during the burning phase. As with other aerodynamic coefficients, values of this coefficient are given by polynomial functions of Mach number of fourth degree or less.

c. The characteristic flow rate function of the base-burn motor is given as follows:

$$f(I) = I/I_0 \quad \text{If } I \le I_0 \tag{D.12}$$

$$f(I) = 1 \quad \text{If } I \ge I_0 \tag{D.13}$$

where: *I* is the base-burn motor fuel injection parameter

$$I = \frac{4\,\dot{m}_f}{\pi\, d_b^{\,2}\, \rho\, v}, \qquad \text{(D.14)}$$

and I_0 is the injection parameter permitting optimum efficiency of the base-burn motor. It is given as a function of Mach number.

NOTE: The function $f(I) = I/I_0$ is principally used for emptying phase and eventually at the start of the burning phase.

d. The coefficient i_{BB} is a fitting factor which can be used, if necessary, to adjust the drag reduction.

e. Mass of the projectile is given by:

for $0 \leq t < t_{DI}$

$$m = m_0 - m_{CB_0} \qquad \text{(D.15)}$$

for $t_{DI} \leq t$ and $m \geq m_B$

$$\dot{m} = \dot{m}_f \qquad \text{(D.16)}$$

$$\dot{m}_f = -V_C\, \rho_p\, S_C\left(m_{CB}\right) \qquad \text{(D.17)}$$

where:

$$m_B = m_0 - m_f \qquad \text{(D.18)}$$

$$m_{CB} = m_0 - m \qquad \text{(D.19)}$$

m_{CB_0} is the mass of fuel burnt in the barrel;

V_C is the combustion rate;

ρ_p is the density of fuel;

$S_C\ (m_{CB})$ is the area of combustion at time t and will be expressed in the form of a function of the mass of fuel burnt:

$$S_C = a_i + b_i\, m_{CB}; \qquad \text{(D.20)}$$

for $m_{CB_i} < m_{CB} \leq m_{CB_{i+1}}$

a_i and b_i are defined over regions of m_{CB}, from $m_{CB_{i=0}}$ up to and including $m_{CB_{i=n}}$.

The combustion rate is given by:

$$V_C = V_{C_0} f(MT) g(P) K(p) \tag{D.21}$$

where:

V_{C_0} is the combustion rate obtained on the strand burner at standard pressure and temperature

MT is the motor fuel temperature

$$f(MT) = e^{\beta(MT-21)} \tag{D.22}$$

P is the local atmospheric air pressure

$$g(P) = k\,P^n \tag{D.23}$$

p is the axial spin of the projectile

K(p) is determined from experiments to take into account the influence of axial spin on the combustion rate, *K(p)* is a linear function of spin for each charge.
The time of motor burnout, t_B, is the time for which $m = m_B$ and it is a program output.

3. Equations II

1. The location of the center of mass for base burn and rocket-assisted projectiles is given by:

$$X_{CG} = X_{CG_0} + \left[\frac{\left(X_{CG_0} - X_{CG_B}\right)\left(m - m_0\right)}{m_0 - m_B}\right] \tag{D.24}$$

2. Common Equations for base burn and rocket-assisted projectiles:

a. The overturning moment coefficient of the munition is given by:

$$C_{M_\alpha} = C^*_{M_\alpha} + \left[\frac{\left(X_{CG} - X_{CG_0}\right)\left(C_{D_0} + C_{L_\alpha}\right)}{d} \right] \tag{D.25}$$

where: $C^*_{M_\alpha}$ is determined for the initial munition configuration and, when $t_{DI} \leq t < t_B$, then C_{D_0} equals $C_{D_{0_T}}$ for rocket-assisted projectiles and fin-stabilized rockets.

b. The cubic overturning moment coefficient of the munition is given by:

$$C_{M_{\alpha^3}} = C^*_{M_{\alpha^3}} + \left[\frac{\left(X_{CG} - X_{CG_0}\right)\left(C_{L_{\alpha^3}} + C_{D_{\alpha^2}} - 1/2\, C_{L_\alpha}\right)}{d} \right] \tag{D.26}$$

where: $C^*_{M_{\alpha^3}}$ is determined for the initial munition configuration.

c. The axial moment of inertia of the munition is given by:

$$I_x = I_{x_0} + \left[\frac{\left(I_{x_0} - I_{x_B}\right)\left(m - m_0\right)}{m_0 - m_B} \right] \tag{D.27}$$

3. The location of the center of mass, motor nozzle exit, motor nozzle throat, and transverse moment of inertia for fin-stabilized rockets.

a. The location of the center of mass is given by:

$$X_{CG} = X_{CG_B} + \left[\frac{\left(X_{CG_{f0}} - X_{CG_B}\right)\left(m - m_B\right)}{m} \right] \tag{D.28}$$

where:

$$X_{CG_{f0}} = X_{CG_B} + \frac{(X_{CG_0} - X_{CG_B})m_0}{(m_0 - m_B)}$$

b. The location of the motor nozzle exit from the center of the mass is given by:

$$r_e = \ell - X_{CG} \tag{D.29}$$

c. The location of the motor nozzle throat from the center of mass is given by:

$$r_t = r_e - r_{t-t} \tag{D.30}$$

d. The transverse moment of inertia of a fin-stabilized rocket is given by:

$$I_Y = I_{Y_0} - (m_0 - m) r_f^2 + m_0 \left(X_{CG_{f0}} - X_{CG_0} \right)^2 - m \left(X_{CG_f} - X_{CG} \right)^2 \tag{D.31}$$

where: r_f is the radius of gyration of the fuel mass.

Figure D.1 illustrates the distances used for the determination of the transverse moment of inertia of the rocket or projectile during motor burning.

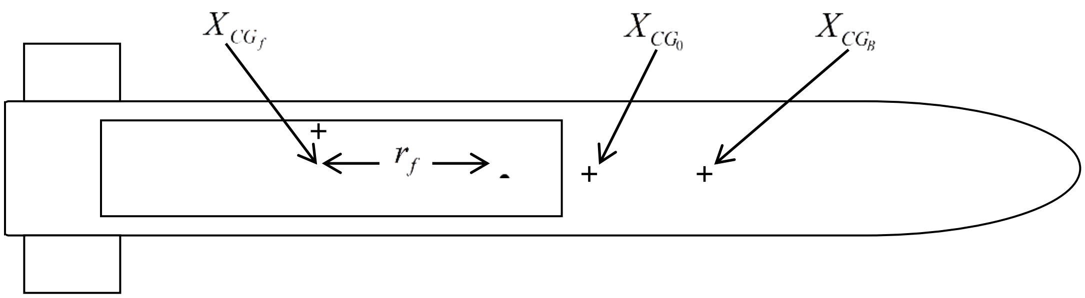

Figure D.1: Distances Used for the Determination of the Transverse Moment of Inertia

4. List of Symbols

Symbol	Definition	Unit
A_e	Exit area of jet m^2	
a_i	Coefficient (constant)	-
b_i	Coefficient (constant)	-
$\overrightarrow{BB}$	Acceleration due to drag reduction of base-burn motor	m/s^2
$C_{D_{0_T}}$	Zero yaw drag coefficient (thrust on)	-
$C^*_{M_\alpha}$	Overturning moment coefficient for initial projectile configuration	-
$C_{x_{bb}}$	Drag reduction coefficient during base-burn motor burning	-
d	Reference diameter of projectile	m
d_b	Diameter of projectile base	m
e	Base of natural logarithms	-
$f(i_{BB,\ MT})$	Base-burn factor	-
$f(I)$	Function I -	
$f(MT)$	Combustion rate as a function of motor fuel temperature	-
f_T	Thrust Factor -	
$g(P)$	Combustion rate as a function of atmospheric air pressure	-
i_{BB}	Fitting factor to adjust the drag reduction as a function of quadrant elevation	-
I	Base-burn motor fuel injection parameter	-

I_0	Base-burn motor fuel injection parameter for optimum efficiency	-
I_{SP}	Specific impulse	*Ns/kg*
I_x	Axial moment of inertia of the projectile	$kg\ m^2$
I_{x_0}	Initial axial moment of inertia	$kg\ m^2$
I_{x_B}	Axial moment of inertia at burnout	$kg\ m^2$
I_y	Transverse moment of inertia	$kg\ m^2$
I_{y_0}	Initial transverse moment of inertia	$kg\ m^2$
k	Constant in burning rate versus pressure formula	-
$K(p)$	Axial spin burning rate factor	-
ℓ	Distance of the motor nozzle exit from nose	*m*
m_0	Initial fuzed projectile mass	*kg*
m_B	Fuzed projectile mass at burnout	*kg*
m_{CB}	Mass of motor fuel burnt	*kg*
m_{CB_0}	Mass of motor fuel burnt in the barrel	*kg*
m_{DI}	Ignition delay element mass	*kg*
m_{DOB}	Delay obturator mass	*kg*
m_f	Projectile fuel mass	*kg*
$\dot{m}_f$	Mass flow rate of the motor fuel	*kg/s*
MT	Temperature of motor fuel	°*C*
n	Exponent in burning rate versus pressure formula	-

P	Air pressure *Pa*	
P_r	Reference air pressure for standard thrust	*Pa*
r_e	Distance from the body center-of-mass to the motor nozzle exit	*m*
r_f	Radius of gyration of the motor fuel mass	*m*
r_t	Distance from the body center-of-mass to the motor nozzle throat	*m*
$r_{t\text{-}t}$	Distance of the motor nozzle exit from the motor nozzle throat	*m*
S_C	Area of combustion at time t	m^2
t	Computed time of flight	*s*
t^*	Pseudo-computed time for mapping of thrust at nonstandard conditions	*s*
t_B	Time of rocket motor burnout	*s*
$t_{B_{ST}}$	Standard time of rocket motor burnout	*s*
t_{DI}	Time of rocket motor ignition delay	*s*
$t_{DI_{ST}}$	Standard time of rocket motor ignition delay	*s*
T_R	Thrust produced by rocket motor at time t	*N*
T_{ST}	Standard thrust as function of burning time	*N*
T^*	Effective thrust *N*	
V_C	Combustion rate of base-burn fuel	*m/s*
V_{C_0}	Combustion rate of base-burn fuel on strand burner	*m/s*
X_{CG}	Distance of center of mass from nose at time t	*m*

X_{CG_0}	Initial distance of center of mass from nose	*m*
X_{CG_B}	Distance of center of mass from nose at burnout	*m*
$X_{CG_{f0}}$	Distance of center-of-mass of the rocket motor fuel from nose, initially	*m*
β	Base-burn motor temperature fuel burning coefficient	-
ρ_p	Density of base-burn motor fuel	kg/m^3

5. Additional Data Requirements

Additional Data Requirements for Rocket-Assisted and Base-Burn Projectiles

(1) Physical Data	*Symbol*
Exit area of jet	A_e
Reference diameter of projectile	d
Axial moment of inertia of the projectile	I_x
Initial axial moment of inertia of the projectile	I_{x_0}
Axial moment of inertia of the projectile at motor burnout	I_{x_B}
Transverse moment of inertia of the rocket, initially	I_{Y_0}
Distance of the motor nozzle exit from nose	ℓ
Fuzed projectile mass at burnout	m_B
Initial mass of fuzed projectile	m_0
Radius of gyration of motor fuel mass	r_f
Distance of the motor nozzle exit from the motor nozzle throat	$r_{t\text{-}t}$
Initial distance of center of mass from nose	X_{CG_0}
Distance of center of mass from nose at burnout	X_{CG_B}

(2) Aerodynamic Data	*Symbol*
Zero Yaw drag coefficient (thrust on)	$C_{D_{0_T}}$
Overturning moment coefficient for initial fuzed projectile	$C^*_{M_\alpha}$
Drag reduction coefficient during base-burn motor burning	$C_{x_{BB}}$

(3) Motor Data – Rocket-Assisted	*Symbol*
Specific impulse	I_{SP}
Ignition delay element mass	m_{DI}
Delay obturator mass	m_{dob}
Mass of rocket motor fuel	m_f
Reference air pressure for standard thrust	P_r
Time of rocket motor burnout	t_B
Standard time of motor burnout	$t_{B_{ST}}$
Time of rocket motor ignition delay	t_{DI}
Standard time of rocket motor ignition delay	$t_{DI_{ST}}$
Standard thrust as function of pseudo-time	T_{ST}

(4) Motor Data – Base-Burn	*Symbol*
Base-burn motor fuel injection parameter for optimum efficiency	I_0

Mass of fuel burnt in the barrel	m_{CB_0}
Mass of motor fuel	m_f
Area of combustion expression in the form of a function of the mass of fuel burnt $S_C = a_i + b_i\, m_{CB}$; for $m_{CB_i} < m_{CB} \leq m_{CB_{i+1}}$ a_i and b_i are defined over regions of m_{CB}, from $m_{CB_{i=0}}$ up to and including $m_{CB_{i=n}}$	S_C
Combustion rate of base-burn fuel on strand burner	V_{C_0}
Base-burn motor temperature fuel burning coefficient	β
Exponent in burning rate versus pressure formula	n
Density of base-burn motor fuel	ρ_p
Constant in burning rate versus pressure formula	k

ANNEX E ADDITIONAL TERMS FOR ROCKET-ASSISTED AND BASE-BURN PROJECTILES-METHOD 2

1. Introduction

This annex provides the equations required to simulate the flight of rocket-assisted projectiles and the specific equations required to simulate the flight of base-burn projectiles. This method is fully defined in ANNEX D to STANAG 4355. Basically, the differences are due to the use of body-fixed axes in the 6/7 DOF simulation rather than wind axes. That is, the body-fixed axes coordinates are X forward along body rotational symmetry axis, Y rightward, and the third axis Z completes a right hand set.

2. Equations I

1. The acceleration due to thrust of the rocket motor, T^*, during burning ($t_{DI} \leq t \leq t_B$) is added to the F_X/m term in the projectile's body-fixed or zero-p frame in the equation of motion of the center of mass of the unassisted projectile. The components F_Y and F_Z in the body-fixed frame are unaffected.

$$T^* = \left[\frac{f_T \, \dot{m}_f \, I_{SP} + \left(P_r - P\right) A_e}{m} \right] \tag{E.1}$$

During rocket motor burning, if $\dot{m}_f \leq \dot{m}_P$ then $(P_r - P)\, A_e = 0$. The aerodynamic zero-yaw coefficient is changed to C_{D0_T} during rocket motor burning. This is accomplished by having a new stage in the simulation and reading in a new table for this aerodynamic coefficient.

2. The base drag reduction due to a base-burn motor during burning ($t_{DI} \leq t \leq t_B$) is added to the F_X/m term in the projectile's body-fixed or zero-p frame in the equation of motion of the center of mass of the unassisted projectile. The components F_Y and F_Z in the body-fixed frame are unaffected.

$$\text{base drag reduction} = -\frac{i}{m}\frac{1}{2}\rho S \left\{ -f\left(i_{BB,MT}\right) \left[\frac{I\left(\frac{\delta BP}{\delta I}\right)}{\left(\frac{\gamma}{2}\right) M^2 \left(\frac{d}{d_b}\right)^2} \right] \right\} v^2 \tag{E.2}$$

where:

$$I = \frac{4\dot{m}_f}{\pi \rho v d_b^{\,2}} \tag{E.3}$$

3. Equations II

1. Common Equations for base-burn and rocket-assisted, spin-stabilized projectiles, and fin-stabilized rockets.

   a. The mass flow for spin-stabilized projectiles and fin-stabilized rockets is given by:

at $t = 0$

$$m = m_0 \tag{E.4}$$

$$\dot{m} = 0 \tag{E.5}$$

for $0 < t < t_{DI}$

$$\dot{m} = -\frac{m_{DI}}{t_{DI}} \tag{E.6}$$

$$m = -\int_0^{t_{DI}} \left(\frac{m_{DI}}{t_{DI}}\right) dt + m_0 \tag{E.7}$$

for $t_{DI} \leq t < t_B$

$$\dot{m} = -\dot{m}_f \tag{E.8}$$

$$m = -\int_{t_{DI}}^{t_B} \dot{m}_f \; dt - \int_0^{t_{DI}} \left(\frac{m_{DI}}{t_{DI}}\right) dt + m_0 \tag{E.9}$$

$$\dot{m}_f = \left(\frac{t_B^* - t_{(t)}^*}{t_{B_{(t)}} - t}\right) \dot{m}_f^* \tag{E.10}$$

$$\dot{t}_{(t)}^* = \frac{t_B^* - t_{(t)}^*}{t_{B_{(t)}} - t} \tag{E.11}$$

$$\dot{t}_{B_{(t)}} = \left(t_{B_{(t)}} - t\right)\left[f_{BT_p} \left(\frac{\dot{p}}{p}\right) + f_{BT_P} \left(\frac{\dot{P}}{P}\right)\right] \tag{E.12}$$

where:

$$\dot{P} = \frac{\Delta P}{\Delta t} = \frac{\Delta P}{\Delta E_2} u_2 \quad \text{(E.13)}$$

and at t_{DI}

$$t^*_{(t_{DI})} = t^*_{DI} \quad \text{(E.14)}$$

$$t_{B_{(t_{DI})}} = t_{DI} + \left[(t_B - t_{DI}) \left(\frac{p_{(t_{DI})}}{p_r} \right)^{f_{BT_p}} \left(\frac{P_{(t_{DI})}}{P_r} \right)^{f_{BT_P}} \right] \quad \text{(E.15)}$$

(Time-of-motor burnout as a function of t_{DI})

p_r	=	Reference axial spin rate for motor mass flow
$p_{(t_{DI})}$	=	Actual spin rate for motor mass flow at t_{DI}
P_r	=	Standard atmospheric air pressure
$P_{(t_{DI})}$	=	Actual atmospheric air pressure at t_{DI}

for $t \geq t_B$

$$m_B = m_0 - m_{DI} - m_f \quad \text{(E.16)}$$

$$\dot{m} = 0 \quad \text{(E.17)}$$

b. The location of the center of mass of the munition is given by:

$$X_{CG} = X_{CG_B} + \left[\frac{(X_{CG_{f0}} - X_{CG_B})(m - m_B)}{m} \right] \quad \text{(E.18)}$$

where:

$$X_{CG_{f0}} = X_{CG_B} + \frac{(X_{CG_0} - X_{CG_B}) m_0}{(m_0 - m_B)} \quad \text{(E.19)}$$

c. The location of the motor nozzle exit from the center of the mass is given by:

$$r_e = \ell - X_{CG} \quad \text{(E.20)}$$

d. The location of the motor nozzle throat from the center of mass is given by:

$$r_t = r_e - r_{t-t} \tag{E.21}$$

e. The overturning moment coefficient of the munition is given by:

$$C_{M_\alpha} = C^*_{M_\alpha} + \left[\frac{\left(X_{CG} - X_{CG_0}\right)\left(C_{D_0} + C_{L_\alpha}\right)}{d} \right] \tag{E.22}$$

where: $C^*_{M_\alpha}$ is determined for the initial munition configuration and, when $t_{DI} \leq t < t_B$, then C_{D_0} equals $C_{D_{0_T}}$ for rocket-assisted projectiles and fin-stabilized rockets. The aerodynamic coefficients are considered to be dimensionless, with unit = 1, in this formulation.

f. The cubic overturning moment coefficient of the munition is given by:

$$C_{M_{\alpha^3}} = C^*_{M_{\alpha^3}} + \left[\frac{\left(X_{CG} - X_{CG_0}\right)\left(C_{L_{\alpha^3}} + C_{D_{\alpha^2}} - 1/2\, C_{L_\alpha}\right)}{d} \right] \tag{E.23}$$

where: $C^*_{M_{\alpha^3}}$ is determined for the initial munition configuration.
The aerodynamic coefficients are considered to be dimensionless, with unit=1, in this formulation.

g. The axial moment of inertia of the munition is given by:

$$I_x = I_{x_0} + \left[\frac{\left(I_{x_0} - I_{x_B}\right)\left(m - m_0\right)}{m_0 - m_B} \right] \tag{E.24}$$

h. The transverse moment of inertia of a fin-stabilized rocket is given by:

$$I_Y = I_{Y_0} - \left(m_0 - m\right) r_f^2 + m_0 \left(X_{CG_{f_0}} - X_{CG_0} \right)^2 - m \left(X_{CG_f} - X_{CG} \right)^2 \tag{E.25}$$

Figure E.1 illustrates the distances used for the determination of the transverse moment of inertia of the rocket during motor burning.

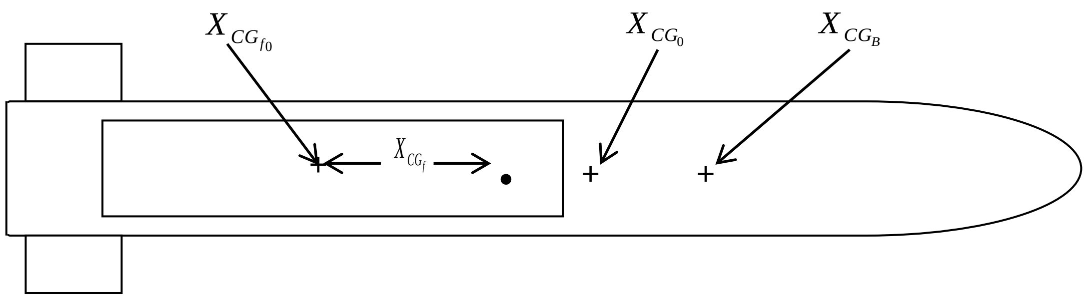

Figure E.1: Distances Used for the Determination of the Transverse Moment of Inertia

4. List of Symbols

Symbol	Definition	Unit
A_b	Area of projectile base	m^2
A_e	Exit area of the motor jet	m^2
C_{D_0}	Zero yaw drag coefficient	-
$C_{D_{0_T}}$	Zero yaw drag coefficient during rocket motor burning	-
$C^*_{M_\alpha}$	Overturning moment coefficient for initial fuzed munition	-
$C^*_{M_\alpha{}^3}$	Cubic overturning moment coefficient for initial fuzed munition	$1/rad^2$
d_b	Diameter of projectile base	m
f_T	Thrust factor	-
$f(i_{BB,\ MT})$	Base-burn factor	-
f_{BT_p}	Base-burn motor spin rate burning-time factor	-
f_{BT_P}	Base-burn motor atmospheric air pressure burning-time factor	-
I	Base-burn motor fuel injection parameter	-
i_{BB}	Fitting factor to adjust the drag reduction as a function of quadrant elevation	-
I_x	Axial moment of inertia of the munition at time t	$kg\ m^2$
I_{x_0}	Axial moment of inertia of the munition, initially	$kg\ m^2$
I_{x_B}	Axial moment of inertia of the munition at motor burnout	$kg\ m^2$

I_Y	Transverse moment of inertia of the rocket at time *t*	*kg m²*
I_{Y_0}	Transverse moment of inertia of the rocket, initially	*kg m²*
ℓ	Distance of the motor nozzle exit from nose	*m*
m_0	Fuzed munition mass, initially	*kg*
m_B	Fuzed munition mass at burnout	*kg*
m_{DI}	Mass of ignition delay element	*kg*
m_f	Mass of motor fuel	*kg*
$\dot{m}_f^*$	Reference mass flow rate of the motor fuel as a function of *t** pseudo-time-of-motor burning	*kg/s*
$\dot{m}_P$	Minimum mass flow rate of the motor fuel for air pressure term	*kg/s*
MT	Temperature of motor fuel	*°C*
p	Axial spin rate of projectile	*rad/s*
p_r	Reference axial spin rate for motor mass flow	*rad/s*
r_e	Distance from the body center-of-mass to the motor nozzle exit	*m*
r_f	Radius of gyration of the motor fuel mass	*m*
r_t	Distance from the body center-of-mass to the motor nozzle throat	*m*
r_{t-t}	Distance of the motor nozzle exit from the motor nozzle throat	*m*
t^*	Pseudo-time-of-motor burning	*s*
t_B	Time-of-motor burnout	*s*

t_B^*	Reference time-of-motor burnout	*s*
t_{DI}	Time-of-motor ignition delay	*s*
t_{DI}^*	Reference time-of-motor ignition delay	*s*
X_{CG}	Distance of center of mass of the munition from nose at time *t*	*m*
X_{CG_0}	Distance of center of mass of the munition from nose at time t_0	*m*
X_{CG_B}	Distance of center of mass of the munition from nose at time t_B	*m*
$X_{CG_{f0}}$	Distance of center-of-mass of the rocket motor fuel from nose at time t_0	*m*
$\frac{\delta BP}{\delta I}$	Change in non-dimensional base pressure for a change in the base-burn motor injection parameter	-
$\frac{\Delta P}{\Delta t}$	Rate of change of atmospheric air pressure as seen by the munition	*Pa/s*

5. Additional Data Requirements

Physical data	***Symbol***
Area of projectile base	A_b
Exit area of motor jet	A_e
Diameter of projectile base	d_b
Axial moment of inertia of the munition, initially	I_{x_0}
Axial moment of inertia of the munition at motor burnout	I_{x_B}
Transverse moment of inertia of the rocket, initially	I_{Y_0}
Distance of the motor nozzle exit from nose	ℓ
Fuzed munition mass, initially	m_0
Fuzed munition mass at burnout	m_B
Mass of ignition delay element	m_{DI}
Mass of motor fuel	m_f
Minimum mass flow rate of the fuel for air pressure term	$\dot{m}_p$
Radius of gyration of motor fuel mass	r_f
Distance of the motor nozzle exit from the motor nozzle throat	$r_{t\text{-}t}$
Distance of center of mass of the munition from nose, initially	X_{CG_0}
Distance of center of mass of the munition from nose at motor burnout	X_{CG_B}

Aerodynamic data	***Symbol***
Zero yaw drag coefficient during rocket motor burning	C_{D0_T}
Overturning moment coefficient for initial fuzed munition	$C^*_{M_\alpha}$
Nonlinear overturning moment coefficient for initial fuzed munition	$C^*_{M_{\alpha^3}}$

Motor data	***Symbol***
Reference mass flow rate of the motor fuel as a function of pseudo-time-of motor burning, *t** $\dot{m}_f^* = a_0 + a_1 t^* + a_2 t^{*2}$; for $t_i^* < t^* \leq t_{i+1}^*$ a_0 and a_1 are defined over regions of t^*, from $t^*_{i=0}$ up to and including $t^*_{i=n}$	$\dot{m}_f^*$
Reference axial spin rate for motor mass flow	p_r
Standard atmospheric air pressure at sea level	P_r
Time-of-motor burnout	t_B
Reference time-of-motor burnout	t_B^*
Time-of-motor ignition delay	t_{DI}
Reference time-of-motor ignition delay	t_{DI}^*
Specific impulse of motor fuel	I_{SP}
Change in non-dimensional base pressure for a change in the base-burn motor injection parameter as a function of Mach number and injection parameter	$\frac{\delta BP}{\delta I}$
Thrust factor	f_T

ANNEX F GUIDED PROJECTILE MODELING

1. Simulation Architecture

Although any part of a simulation source code may be subject to modification, it is expected that basic 6/7 DOF code will be stable and a simulation would adapt to different projectiles by input data files. This stable part of the simulation is shown in blue in Figure F.1. Experience has shown that the part of the code that describes the guidance, navigation and control (GNC) capabilities of the projectile cannot just be written generically but needs to be tailored to various designs. This part is shown in yellow in Figure F.1.

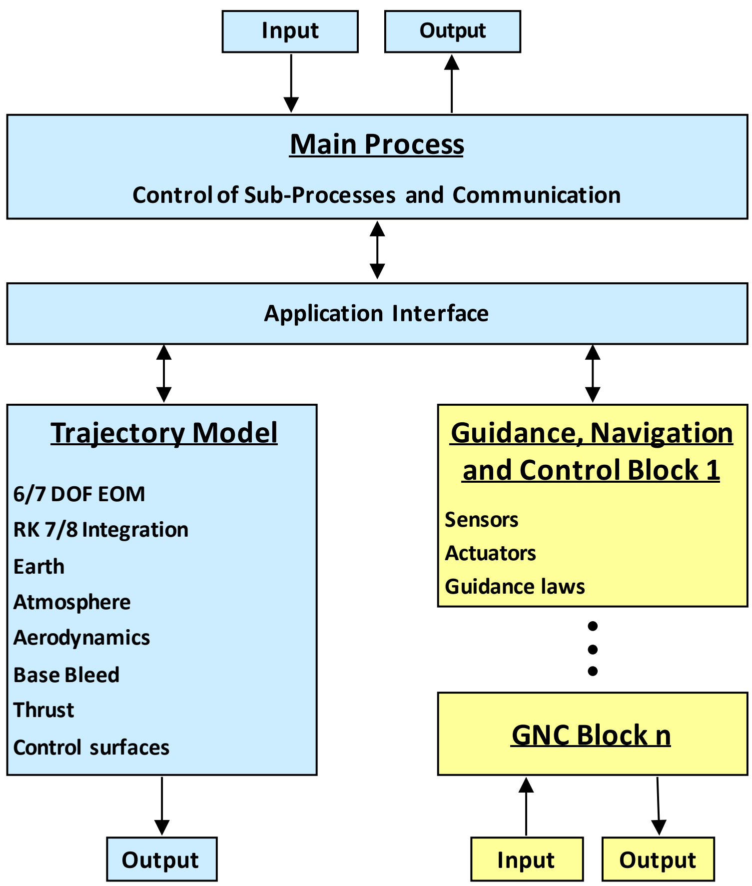

Figure F.1: Overall simulation architecture

Basic 6/7 DOF trajectory code should be usable as a standalone application to compute either unguided trajectories or open-loop controlled trajectories.

A library of models should be made available for GNC blocks: models for sensors and actuators to simulate projectile hardware and models for guidance capabilities. These models should be linked to the 6/7 DOF simulation code by means of a generic application interface. The definition of this interface is part of this Annex.

2. Generic Closed-Loop Architecture

Figure F.2 describes a generic closed-loop architecture where the blocks represent the main functions and the arrows indicate the data flow (dotted arrows are optional data flow). At each cycle of the flight path integration process, the trajectory model must forward the true system state to the GNC block and requests an update of the projectile parameters related to the embedded actuators.

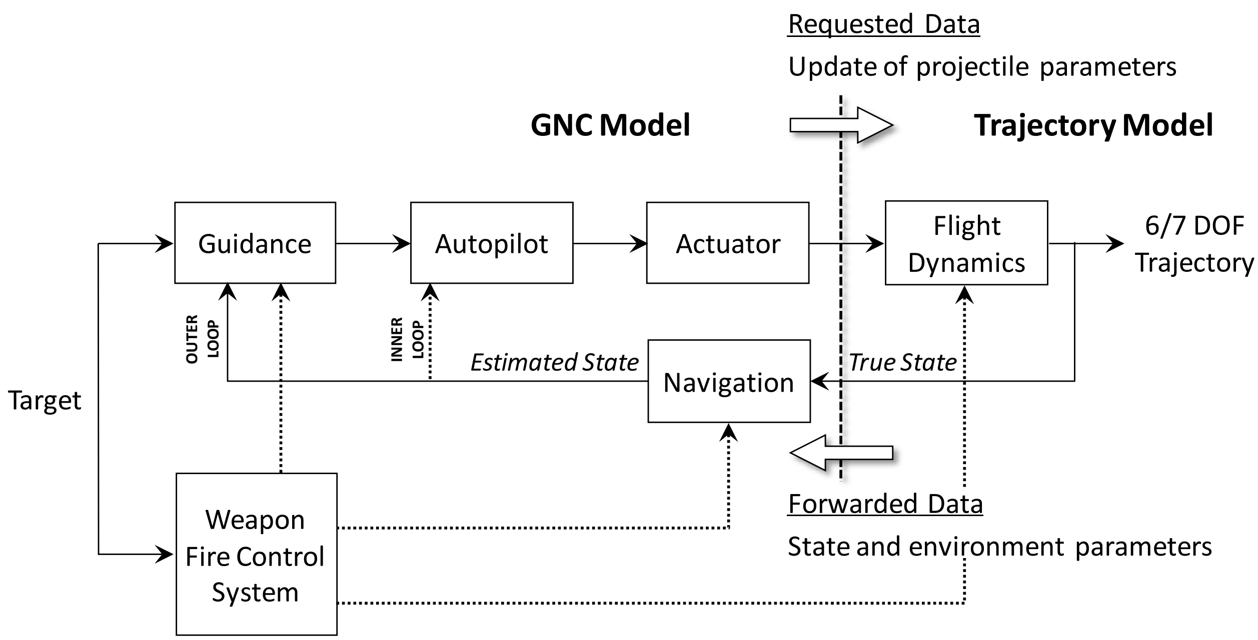

Figure F.2: Generic closed-loop architecture

The outer loop (or guidance loop) controls the translational kinematics of the projectile in order to reach the target. The optional inner loop(s) may control the rotational kinematics of the projectile so that it remains stable. See section 7 about autopilots.

3. Generic Interface

The generic interface described hereafter is the *minimum set of data* that should be transferred between the trajectory model and the GNC model. This set should be extended according to the evolution of the guided ammunition design.

3.1 Data transferred from Trajectory Model to GNC Model

Data	**Dim**	**Unit**
Time of flight	1	s
Rotation matrix: body system to fire control system	3x3	-
Rotation matrix: fire control system to ECEF system	3x3	-
Position of projectile w.r.t. fire position in fire control system	3	m
Position of projectile w.r.t. fire position in surface system	3	m
Position of projectile w.r.t. Earth center in ECEF	3	m
Attitude of body frame w.r.t. fire control system: Quaternion	4	-
Attitude of body frame w.r.t. fire control system: Euler angles (yaw, pitch, roll)	3	rad
Attitude of body frame w.r.t. ECEF: Quaternion	4	-
Attitude of body frame w.r.t. ECEF: Euler angles (yaw, pitch, roll)	3	rad
Velocity of projectile w.r.t. ECEF in fire control system	3	m/s
Angular velocity of body frame w.r.t. ECEF in body system	3	rad/s
Angular velocity of body frame w.r.t. ECI in body system	3	rad/s
Time derivative of angular velocity of body frame w.r.t. ECI in body system	3	rad/s^2
Wind in fire control system	3	m/s
Air density	1	kg/m^3
Speed of sound	1	m/s
Gravity in fire control system	3	m/s^2
Sum of aerodynamic and thrust forces in fire control system	3	N
Sum of aerodynamic, thrust and jet damping moments in fire control system	3	N m
Projectile caliber	1	m
Projectile mass	1	kg
Projectile M.O.I. in body system	3x3	$kg\,m^2$
Number of fins attached to main body (NF)	1	-
Number of thrusters attached to main body (NT)	1	-

3.2 Data transferred from GNC Model to Trajectory Model

Data	Dim	Unit
Projectile mass	1	kg
Projectile M.O.I. in body system	3x3	$kg\,m^2$
Deflection of fins attached to main body	NF	rad
Area of fins attached to main body	NF	m^2
Thrust amplitude due to thrusters attached to main body	NT	N
Contact moment between main body and body 2 (7 DOF model)	1	N m

4 Weapon Fire Control System

The input of the Weapon Fire Control model consists of targeting information:
- Target position;
- Target velocity (in case of moving targets).

The output of the Weapon Fire Control model should be structured into:
- Gun aiming output:
  - Commanded azimuth
  - Commanded elevation (in case of elevation trainable systems)
- Projectile navigation output:
  - Target initialization data
    - Coordinates with respect to a Reference Point
  - Navigation initialization data:
    - Coordinates of the weapon with respect to a Reference Point
    - Initial attitude
  - Guidance initialization
    - Additional data used by the guidance system (e.g. activation time of a drag brake, or terminal approach angle)

5 Navigation

The navigation block includes models of body-fixed sensors such as accelerometers, gyrometers or magnetometers (these are IMU sensors) as well as models of external tracking systems such as the GPS.

5.1 Accelerometer

Let us consider an ideal 3-axis accelerometer fixed to the projectile body frame and displaced from the center of gravity by $\overline{R}$. It is assumed that the 3 axes of the accelerometer are perfectly parallel to the x, y, and z body-axes of the projectile. The sensed acceleration $\overline{A}_S$ is given by

$$\overline{A}_S = \frac{\overline{F}}{m} + \frac{d\overline{\varpi}}{dt} \times \overline{R} + \overline{\varpi} \times \left(\overline{\varpi} \times \overline{R} \right) \quad \text{(F.1)}$$

where $\overline{F}$ is the sum of the aerodynamic and thrust forces, m is the mass of the projectile and $\overline{\varpi}$ is the angular velocity of the projectile. Note that an accelerometer senses all accelerations except the acceleration of gravity.

Limiters may be used to represent saturation of the output of the sensors. Axis misalignments, noise, biases, scale factors, cross-axis coupling and other noise sources are ignored in this idealization. These errors can be handled by specific models.

5.2 Gyrometer

An ideal 3-axis rate gyro is modeled simply as sensing the *p*, *q*, and *r* components of the angular velocity of the projectile given in the body-fixed frame. Limiters may be used to represent saturation of the output of the sensors. Gyro errors can be handled by specific models.

5.3 Magnetometer

An ideal 3-axis magnetometer is modeled simply as sensing the three components of the Earth magnetic field given in the body-fixed frame. Limiters may be used to represent saturation of the output of the sensors. Magnetometers errors can be handled by specific models.

6 <u>Guidance</u>

Guidance refers to a variety of methods of guiding a vehicle to its intended target. Within the frame of this STANAG, the guidance system described by Figure F.2 takes input from the navigation system and uses targeting information to send signals to the flight control system (i.e. the autopilot and actuator blocks) that will allow the projectile to reach its destination.

Proportional navigation (PN) and its variants are some of the most widely used missile guidance laws in the literature. These guidance laws are easy to implement and have shown good performance against non-maneuvering and moderately maneuvering targets.

The basic two dimensional (2D) engagement scheme of proportional navigation is shown in Figure F.3. The amplitude of the lateral acceleration command applied to the projectile is defined by

$$A_C = N V_B \dot{\lambda} \tag{F.2}$$

where N is the navigation ratio, V_B is the projectile velocity and $\dot{\lambda}$ is the time derivative of the projectile-to-target line of sight (LOS) angle λ. The form of PN called pure PN is characterized by the fact that the lateral acceleration command is normal to the projectile velocity vector.

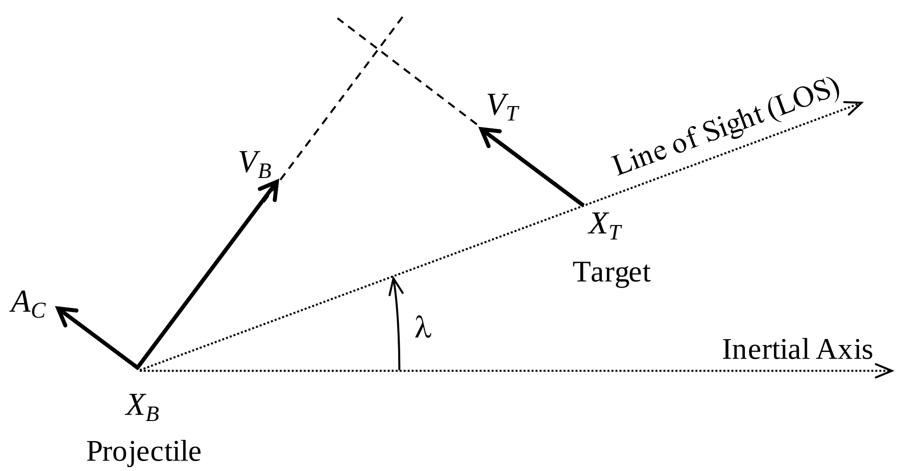

Figure F.3: Proportional navigation scheme

The extension of the 2D PN scheme to the 3D case requires defining the LOS angular velocity vector $\overline{\omega}^{LOS}$ as follows

$$\overline{\omega}^{LOS} = \frac{(\overline{X}_T - \overline{X}_B) \times (\overline{V}_T - \overline{V}_B)}{(\overline{X}_T - \overline{X}_B)^2} \quad \text{(F.3)}$$

Finally, taking into account the influence of the gravity, the acceleration command is given by

$$\overline{A}_C = N\overline{\omega}^{LOS} \times \overline{V}_B - \overline{g}_N \quad \text{(F.4)}$$

where $\overline{g}_N$ is the component of the gravity vector that is normal to the projectile velocity vector.

7 Autopilot

The role of the autopilot depends on the type of projectile. For example, in the case of a roll stabilized frame the autopilot will realize the roll stabilization. In any case, the autopilot translates the commanded lateral acceleration computed by the guidance algorithms to actuation commands for the steering system. In some cases, the autopilot uses inertial measurements of the rotational and translational dynamics of the airframe as an inner loop in the GNC system (as illustrated in Figure F.2). An autopilot using an inner loop may be used to stabilize the frame and to make the response of the airframe to guidance commands less sensitive to flight conditions, and thus improve the performance of the guided projectile. There are however cases in which this latter function is not required and the airframe is steered without the help of the inner loop.

There are several types of autopilots in use for various aerospace applications (see [14] for a general overview). For guided artillery shells, the most relevant types are: lateral acceleration command tracking autopilots, attitude hold autopilots (e.g. roll autopilot), and course following autopilots (for gliding flight).

7.1. Roll Autopilot

For a fin stabilized projectile or missile, the main functionality of the roll autopilot is to roll-stabilize the projectile. Figure F.4 shows a stripped down version of a roll-angle hold autopilot.

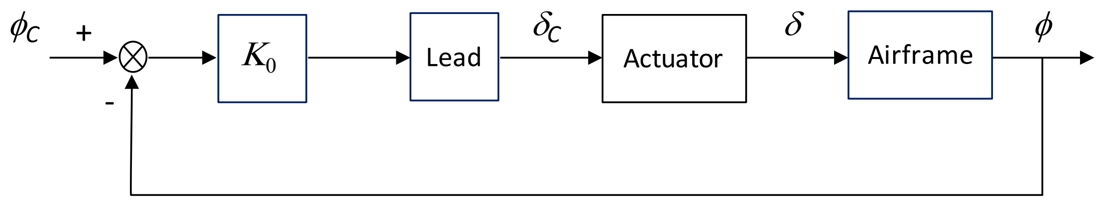

Figure F.4: Simple roll autopilot

The airframe can be described by the second order transfer function

$$\frac{\phi(s)}{\delta(s)} = \frac{k_1}{k_2 s^2 - k_3 s} = \frac{C_{l_\delta}}{s\left(\frac{I_x}{\bar{q}Sd}s - \frac{d}{2V}C_{l_p}\right)} \tag{F.5}$$

where $\bar{q}Sd\delta C_{l_\delta}$ is the roll moment generated by the deflection of the control surfaces.

A generic model of actuator is described in section 8. A lead block has been added for loop shaping purposes. An alternative approach is to include feedback from a roll-rate gyro. The transfer function for the lead block is given by

$$H(s) = \frac{s - z_0}{s - p_0} \tag{F.6}$$

where z_0 and p_0 are the zeros and poles of the transfer function. Together with the gain K_0, desired gain and stability margins can be achieved.

7.2.2 Three-Loop Autopilot

The three-loop autopilot is a classical controller topology used in missile flight control systems, in particular for control of acceleration in the pitch and yaw planes of skid-to-turn operated missiles or fin stabilized projectiles.

7.2.1. Equations of Motion

Consider a fin stabilized projectile in standard configuration (slender, essentially cylinder symmetric with tail fins or canard control) with a body frame *B* with standard orientation. For this case it is customary to set the roll rate *p* to 0 in the Newton-Euler equations (NE) and linearize around zero angle of attack α, sideslip angle β and control surface deflections *δ*. By doing this, and performing various other simplifications based on qualitative and quantitative aspects of the aerodynamic forces and moments, the NE equations decouple into two systems of equations of the same form for the pitch and yaw plane dynamics. It is therefore sufficient to consider only the resulting pitch plane dynamics.

7.2.1.1. Simplified linear pitch plane model

The simplified pitch plane dynamics for α, q can be written

$$\dot{\alpha} = \frac{Z_\alpha}{V}\alpha + \frac{Z_\delta}{V}\delta + q + \frac{F_{z,b}(0,0)}{mV} \quad \text{(F.7)}$$

$$\dot{q} = M_\alpha \alpha + M_q q + M_\delta \delta \quad \text{(F.8)}$$

where V is the (magnitude of the) airspeed, m is the mass of the projectile and δ is the control surface deflection angle.
The quantities Z_α, Z_δ, M_α, M_q, M_δ are normalized force and moment (derivative) terms

$$Z_\alpha = \frac{1}{m}\frac{\partial F_{z,b}(\alpha,\delta)}{\partial \alpha}\bigg|_{(\alpha,\delta)=(0,0)} \quad \text{(F.9)}$$

$$Z_\delta = \frac{1}{m}\frac{\partial F_{z,b}(\alpha,\delta)}{\partial \delta}\bigg|_{(\alpha,\delta)=(0,0)} \quad \text{(F.10)}$$

$$M_\alpha = \frac{1}{I_{yy}}\frac{\partial M_{y,b}(\alpha,q,\delta)}{\partial \alpha}\bigg|_{(\alpha,q,\delta)=(0,0,0)} \quad \text{(F.11)}$$

$$M_q = \frac{1}{I_{yy}}\frac{\partial M_{y,b}(\alpha,q,\delta)}{\partial q}\bigg|_{(\alpha,q,\delta)=(0,0,0)} \quad \text{(F.12)}$$

$$M_\delta = \frac{1}{I_{yy}}\frac{\partial M_{y,b}(\alpha,q,\delta)}{\partial \delta}\bigg|_{(\alpha,q,\delta)=(0,0,0)} \quad \text{(F.13)}$$

derived from the force $F_{z,b}$ along the body *z*-axis and the moment $M_{y,b}$ around the body *y*-axis, where I_{yy} is the moment of inertia about the *y*-axis. The term $F_{z,b}(0,0)$ contains the force due to gravity.

7.2.1.2. Acceleration

The normal acceleration $a_{z,b}$ (along the *z*-axis) in *B* is defined as

$$a_{z,b} = \frac{F_{z,b}(\alpha,\delta)}{m} \qquad \text{(F.14)}$$

and the linearized version of (F.14) reads

$$a_{z,b} = Z_\alpha \alpha + Z_\delta \delta + \frac{F_{z,b}(0,0)}{m} \qquad \text{(F.15)}$$

7.2.1.3. Dynamics

The linearized acceleration dynamics are easily derived from (F.7) and (F.15) as

$$\dot{a}_{z,b} = Z_\alpha \dot{\alpha} + Z_\delta \dot{\delta} + \frac{\dot{F}_{z,b}(0,0)}{m} = \frac{Z_\alpha}{V} a_{z,b} + Z_\alpha q + Z_\delta \dot{\delta} + \frac{\dot{F}_{z,b}(0,0)}{m} \qquad \text{(F.16)}$$

If the projectile flies with a slowly varying Euler pitch angle it is reasonable to neglect the rightmost term in (F.16). For equation (F.8) one obtains similarly

$$\dot{q} = \frac{M_\alpha}{Z_\alpha} a_{z,b} + M_q q + \left(M_\delta - \frac{M_\alpha Z_\delta}{Z_\alpha} \right) \tilde{\delta} \qquad \text{(F.17)}$$

where $\tilde{\delta} = \delta - \delta_0$ and δ_0 is defined by

$$\delta_0 = \frac{M_\alpha F_{z,b}(0,0)}{m(M_\delta Z_\alpha - M_\alpha Z_\delta)} \qquad \text{(F.18)}$$

i.e. δ_0 yields equilibrium (“trim”) in (F.8) when expressed in terms of acceleration and pitch rate.

7.2.2 Three-Loop Autopilot Topology and Transfer function

The three-loop autopilot topology is used in many practical implementations of missile autopilots (not only for acceleration control). In its standard (acceleration control) formulation it employs linear acceleration and angular rate measurements to implement, effectively, a pole placement controller with an extra degree of freedom which can be used to increase robustness. A basic variant of the three-loop controller is depicted in Figure F.5 where the three loops and variables are named.

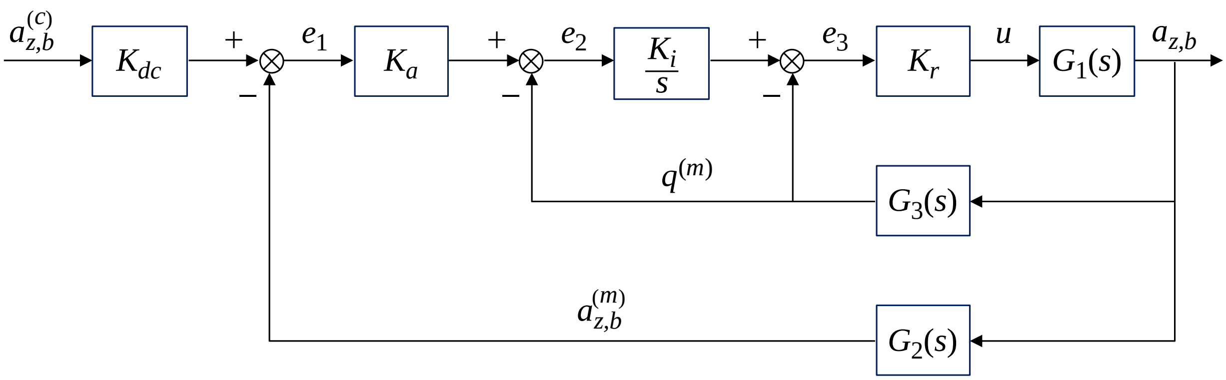

Figure F.5: Three-loop autopilot based on acceleration and angular velocity measurements

The transfer function G_1 represents the bare airframe dynamics, G_2 is the transfer function from acceleration to measured pitch rate and G_3 is the transfer function from acceleration to measured acceleration. The three loops are called the *rate damping loop* (innermost, with error e_3 and gain K_r), *synthetic stability loop* (middle, with error e_2 and integrator with gain K_i) and *accelerometer loop* (outermost, with error e_1 and gain K_a). The control signal u is the control surface deflection δ or the differential deflection $\tilde{\delta} = \delta - \delta_0$ relative to a reference deflection δ_0.

From Figure F.5, one obtains the following relations

$$e_1 = K_{dc} a_{z,b}^{(c)} - a_{z,b}^{(m)} \quad \text{(F.19)}$$

$$e_2 = K_a e_1 - q^{(m)} \quad \text{(F.20)}$$

$$e_3 = \frac{K_i}{s} e_2 - q^{(m)} \quad \text{(F.21)}$$

$$u = K_r e_3 \tag{F.22}$$

$$a_{z,b} = G_1(s)\, u \tag{F.23}$$

$$q^{(m)} = G_3(s)\, a_{z,b} \tag{F.24}$$

$$a_{z,b}^{(m)} = G_2(s)\, a_{z,b} \tag{F.25}$$

7.2.2.1 Closed loop transfer function

By eliminating variables in (F19)–(F25) the closed loop transfer function *H* for the three-loop autopilot is obtained as

$$H(s) = \frac{a_{z,b}}{a_{z,b}^{(c)}} = \frac{K_{dc} K_r \left(\frac{K_i}{s}\right) K_a G_1(s)}{1 + K_r \left(\frac{K_i}{s}\right) K_a G_1(s) G_2(s) + K_r \left(\frac{K_i}{s}\right) G_1(s) G_3(s) + K_r G_1(s) G_3(s)} \tag{F.26}$$

Assuming that ideal measurements are used so that $a_{z,b}^{(m)} = a_{z,b}$ and $q^{(m)} = q$ then $G_2(s) = 1$ and *H* can be written on the form

$$H(s) = K_{dc} K_a K_i K_r \frac{A(s)}{s^3 + b_2 s^2 + b_1 s + b_0} \tag{F.27}$$

where *A* is a second degree polynomial. The four constants K_{dc}, K_a, K_i, K_r can be selected so as to give *H* the desired pole locations (a real pole and a complex conjugate pole pair) as well as the desired static gain *H*(0).

7.2.2.2 Vanishing control surface force contribution

In the limiting case of vanishing Z_δ (which is a good approximation for many tail or canard controlled missiles and projectiles), it is easy to see how to shape the closed loop response *H*. In this case $A(s) = M_\delta Z_\alpha$ and it follows from (F.16), (F.17) and (F.26), (F.27) that

$$b_2 = K_r M_\delta - \frac{Z_\alpha}{V} - M_q \tag{F.28}$$

$$b_1 = \frac{Z_\alpha M_q}{V} - M_\alpha + K_r M_\delta \left(K_i + \frac{Z_\alpha}{V} \right) \tag{F.29}$$

$$b_0 = K_i K_r M_\delta Z_\alpha \left(K_a - \frac{1}{V} \right) \tag{F.30}$$

The static gain becomes

$$H(0) = K_{dc} \frac{K_a}{K_a - \frac{1}{V}} \tag{F.31}$$

Desired values of b_2, b_1, b_0 and $H(0)$ can be obtained (recursively) selecting K_{dc}, K_a, K_i, K_r. It is then worth noting that the gain crossover angular frequency ω_{cr} of the innermost loop, the rate damping loop, is approximately

$$\omega_{cr} = \left| K_r M_\delta \right| \tag{F.32}$$

8. Actuator

A generic actuator can be modeled using a second order differential equation including the possibility to limit the rate and response of the system. Thus, the actuator system is equivalent to a damped harmonic oscillator. Figure F.6 depicts the second order block diagram of a generic fin actuator system.

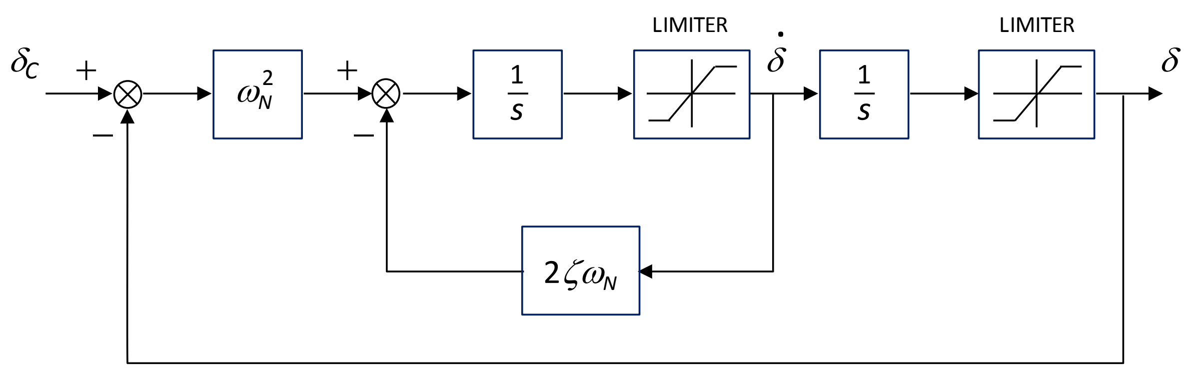

Figure F.6: Block diagram of fin actuator

The transfer function is

$$\frac{\delta(s)}{\delta_C(s)} = \frac{\omega_N^2}{s^2 + 2\zeta\omega_N s + \omega_N^2} \tag{F.33}$$

The corresponding response in the time-domain can be computed using the following integration scheme

$$\begin{cases} \ddot{\delta}_{i+1} = (\omega_N^2(\delta_c - \delta_i) - 2\zeta\omega_N\dot{\delta}_i) \\ \dot{\delta}_{i+1} = \dot{\delta}_i + \Delta t\ddot{\delta}_{i+1} \\ \delta_{i+1} = \delta_i + \Delta t\dot{\delta}_{i+1} \end{cases} \tag{F.34}$$

The one step integration method used in (F.34) is crude but the response is quite reasonable if the system time constant is one or two magnitudes larger than the time step Δt.

9. List of Symbols

Symbol	Definition	Unit
$\bar{A}_C$	Lateral acceleration command	m/s^2
$\bar{A}_S$	Sensed acceleration	m/s^2
$a_{z,b}$	Acceleration along z-axis in body-fixed system	m/s^2
$a_{z,b}^{(c)}$	Acceleration command along z-axis in body-fixed system	m/s^2
$a_{z,b}^{(m)}$	Measured acceleration along z-axis in body-fixed system	m/s^2
Cl_{δ}	Fin cant moment coefficient	-
Cl_p	Spin damping moment coefficient	-
d	Caliber of the projectile	m
e_1, e_2, e_3	Errors (three-loop autopilot)	-
$\bar{F}$	Sum of aerodynamic and thrust forces	N
G_1, G_2, G_3	Transfer functions (three-loop autopilot)	-
H	Closed loop transfer function	-
$\bar{g}_N$	Component of the gravity vector that is normal to the projectile velocity vector	m/s^2
I_x	Moment of inertia about x-axis of the projectile	$kg\,m^2$
I_{yy}	Moment of inertia about y-axis	$kg\,m^2$
K_{dc}, K_a, K_i, K_r	Gain constants (three-loop autopilot)	-

m	Mass of the projectile	*kg*
N	Navigation ratio	-
p	Spin rate	*rad/s*
q	Pitch rate	*rad/s*
$q^{(m)}$	Measured pitch rate	*rad/s*
$\bar{q}$	Dynamic pressure	*Pa*
$\bar{R}$	Displacement w.r.t. the projectile center of gravity	*m*
S	Cross section of the projectile	m^2
s	Frequency variable (Laplace transform)	*1/s*
V	Airspeed	*m/s*
$\bar{V}_B$	Velocity of the projectile	*m/s*
$\bar{V}_T$	Velocity of the target	*m/s*
$\bar{X}_B$	Position of the projectile	*m/s*
$\bar{X}_T$	Position of the target	*m/s*
α	Pitch angle	*rad*
δ	Fin deflection	*rad*
δ_C	Fin deflection command	*rad*
Δt	Time step	*s*
λ	Projectile-to-target line of sight (LOS) angle	*rad*
ϕ	Roll angle	*rad*

ϕ_C	Roll angle command	*rad*
ζ	System damping ratio	-
$\overline{\omega}$	Angular velocity of the projectile	*rad/s*
$\overline{\omega}^{LOS}$	LOS angular velocity	*rad/s*
ω_N	System natural angular frequency	*rad/s*

INTENTIONALLY BLANK

ANNEX G NUMERICAL INTEGRATION

A numerical integration scheme is required because the equations described in this STANREC are too complex for analytical or closed form solution. A 7^{th} order Runge-Kutta-Fehlberg scheme with 8^{th} order error estimation will be used. See selected bibliography in Annex H.

As far as the integration time step is concerned, two methods are available: either keeping the time step constant or adjusting the time step by means of the error estimation. Adjusting the time step is useful to keep down computer run time.

As far as the integration of the quaternion is concerned, no renormalization of the quaternion should be applied. As a matter of fact, checking the evolution of the norm gives some insight of the quality of the integration process.

INTENTIONALLY BLANK

ANNEX H SELECTED BIBLIOGRAPHY

Classical Mechanics

[1] Landau, L. D., Lifshitz, E. M., "Classical Mechanics", Addison Wesley, 1960

[2] Baruh, H., "Analytical Dynamics", McGraw-Hill, 1999

[3] Goldstein, H., Poole, C., Safko, J. L., "Classical Mechanics", Addison Wesley, 3rd Ed., 2001

Exterior Ballistics

[4] Molitz, H., Strobel, R., "Äußere Ballistik", Springer-Verlag, 1963

[5] Murphy, C. H., "Free Flight Motion of Symmetric Missiles", BRL report 1216, July 1963

[6] "Textbook of Ballistics and Gunnery", Volumes I and II, Her Majesty's Stationery Office, London, 1987

[7] Lieske, R. F., Danberg, J. E., "Modified Point Mass Trajectory Simulation for Base-Burn Projectiles", BRL Report No. 3321, U.S. Army Ballistic Research Laboratory, Aberdeen Proving Ground, MD, March 1992

[8] Amoruso, M. J., "Euler Angles and Quaternions in Six Degree of Freedom Simulations of Projectiles", ARDEC report, March 1996

[9] Fleck, V., "Introduction à la balistique extérieure avec exercices", Cours de balistique extérieure, École de Saint-Cyr Coëtquidan, France, 1998

[10] McCoy, R. L., "Modern Exterior Ballistics – The Launch and Flight Dynamics of Symmetric Projectiles", Schiffer Publishing Ltd., 1999

Flight Dynamics, Guidance and Control

[11] Blakelock, J. H., "Automatic Control of Aircraft and Missiles", 2nd Ed., John Wiley & Sons, 1991

[12] Etkin, B., Reid, L. D., "Dynamics of Flight – Stability and Control", 3rd Ed., John Wiley & Sons, 1996

[13] Stengel, R. F., "Flight Dynamics", Princeton University Press, 2004

[14] Zipfel, P. H., “Modeling and Simulation of Aerospace Vehicle Dynamics”, 2nd Ed., AIAA Education Series, 2007

[15] Jackson, P. B., “Overview of Missile Flight Control Systems”, Johns Hopkins APL Technical Digest, Volume 29, Number 1, 2010

Norms

[16] ISO 1151-1, “Flight Dynamics – Concepts, Quantities and Symbols – Part 1: Aircraft Motion Relative to the Air”, Fourth Edition, 1988

[17] AIAA/ANSI R-004-1992, “Recommended Practice for Atmospheric and Space Flight Vehicle Coordinate Systems”, 1992

Other Reference Documents

[18] “American Standard Letter Symbols for Aeronautical Sciences”, ASA Y 10.7, 1954

[19] Fehlberg, E., “Classical Fifth-, Sixth-, Seventh-, and Eighth-Order Runge-Kutta Formulas with Stepsize Control”, NASA TR R-287, 1968 (available on the Internet)

[20] Press, W. H., *et al.*, “Numerical Recipes in Fortran 90”, Cambridge University Press, 1996

[21] “Department of Defense World Geodetic System 1984 – Its Definition and Relationships With Local Geodetic Systems”, Third Edition, NIMA Technical Report TR8350.2, 4 July 1997

[22] Kuipers, J. B., “Quaternions and Rotation Sequences – A Primer with Applications to Orbits”, Aerospace and Virtual Reality, Princeton University Press, 1999

INTENTIONALLY BLANK

AEP-96 (A)(1)